GENETIC DISSECTION OF THE TRANSCRIPTIONAL HYPOXIA RESPONSE AND GENOMIC REGIONAL CAPTURE FOR MASSIVELY PARALLEL SEQUENCING

by

DOUGLAS WILLIAM TURNBULL

A DISSERTATION

Presented to the Department of Biology
and the Graduate School of the University of Oregon
in partial fulfillment of the requirements
for the degree of
Doctor of Philosophy

September 2008

University of Oregon Graduate School

Confirmation of Approval and Acceptance of Dissertation prepared by:

Douglas Turnbull

Title:

"Genetic Dissection of the Transcriptional Hypoxia Response and Genomic Regional Capture for Massively Parallel Sequencing"

This dissertation has been accepted and approved in partial fulfillment of the requirements for the Doctor of Philosophy degree in the Department of Biology by:

Karen Guillemin, Chairperson, Biology
Eric Johnson, Advisor, Biology
Bruce Bowerman, Member, Biology
Christopher Doe, Member, Biology
Kenneth Prehoda, Outside Member, Chemistry

and Richard Linton, Vice President for Research and Graduate Studies/Dean of the Graduate School for the University of Oregon.

September 6, 2008

Original approval signatures are on file with the Graduate School and the University of Oregon Libraries.

An Abstract of the Dissertation of

Douglas William Turnbull for the degree of Doctor of Philosophy

in the Department of Biology to be taken September 2008

Title: GENETIC DISSECTION OF THE TRANSCRIPTIONAL HYPOXIA RESPONSE AND GENOMIC REGIONAL CAPTURE FOR MASSIVELY PARALLEL SEQUENCING

Approved: _____

Dr. Eric Johnson, Advisor

When cells are faced with the stress of oxygen deprivation (hypoxia), they must alter their physiology in order to survive. One adaptation cells make during hypoxia entails the transcriptional activation of specific groups of genes as well as the concurrent repression of other groups. This modulation is achieved through the actions of transcription factors, proteins that are directly involved in this transcriptional activation and repression. I studied the transcriptional response to hypoxia in the model organism *Drosophila melanogaster* utilizing DNA microarrays to examine the transcriptomes of five different mutant *Drosophila* strains deficient in the hypoxia-responsive transcription factors *HIF-1, FOXO, NFκB, p53,* and *MTF-1.* By comparing hypoxia responsive gene expression in these mutants to that of wild type flies and subsequently identifying binding sites for each transcription factor near putative target genes, I was able to identify the

transcripts regulated by each transcription factor during hypoxia. I discovered that *FOXO* plays an unexpectedly large role in hypoxic gene regulation, regulating a greater number of genes than any other transcription factor. I also identified multiple interesting targets of other transcription factors and uncovered a potential regulatory link between HIF-1 and FOXO. This study is the most in-depth examination of the transcriptional hypoxia response to date.

I was also involved in additional research on transcriptional stress responses in *Drosophila*. Also included in this dissertation are two papers on which I was the second author. One paper identified a regulatory link between the transcriptional responses to hypoxia and heat-shock. The other examined elevated CO_2 stress (hypercapnia) in *Drosophila,* showing that this stress causes the down-regulation of *NFκB*-dependent antimicrobial peptide gene expression.

My studies of stress responses would not have been possible without well-described mutant fly strains. Another part of my dissertation research involved the creation of a method for characterizing new mutants for future studies. When researchers seek to identify the molecular nature of a mutation that causes an interesting phenotype, they must ultimately determine the specific responsible genomic sequence change. While classical genetic methods and other techniques can easily be used to roughly map the location of a mutation in a genome, regions identified by these means are usually so large that sequencing them to precisely identify the polymorphism is laborious and slow. I have developed a technique that makes sequencing genomic regions of this size much easier. My technique involves capturing genomic regions by hybridization of fragmented genomic target DNA to biotinylated probes generated from fosmid DNA, which are subsequently

immobilized and washed on streptavidin beads. Genomic DNA fragments are then eluted by denaturation and sequenced using the latest generation of massively parallel sequencing technology. I have demonstrated the effectiveness of this approach by sequencing a mutation-containing 336-kilobase genomic region from a *Caenorhabditis elegans* strain. My entire protocol can be completed in two days, is relatively inexpensive, and is broadly applicable to any situation in which one wants to sequence a specific genomic region using massively parallel sequencing.

This dissertation includes both my previously published and my coauthored materials.

CURRICULUM VITAE

NAME OF AUTHOR: Douglas William Turnbull

PLACE OF BIRTH: LaGrande, Oregon

DATE OF BIRTH: March 18th, 1979

GRADUATE AND UNDERGRADUATE SCHOOLS ATTENDED:

University of Oregon, Eugene, Oregon
University of Puget Sound, Tacoma, Washington

DEGREES AWARDED:

Doctor of Philosophy in Biology, 2008, University of Oregon
Bachelor of Science in Biology, 2001, University of Puget Sound

AREAS OF SPECIAL INTEREST:

Gene Regulation
Genomics

PROFESSIONAL EXPERIENCE:

Graduate Research Fellow, Department of Biology, University of Oregon, Eugene, Oregon, 2003-2007

Graduate Teaching Fellow, Department of Biology, University of Oregon, Eugene, Oregon, 2002-2003

GRANTS, AWARDS AND HONORS:

Keck Foundation Training Grant, University of Oregon, 2007-2008

NIH Genetics Training Grant, University of Oregon, 2005-2007

NIH Molecular Biology Training Grant, University of Oregon, 2003-2004

Murdock Summer Research Fellowship, University of Puget Sound, 2000

PUBLICATIONS:

Baird, N.A., D.W. Turnbull, and E.A. Johnson. 2006. Induction of heat shock pathway during hypoxia requires regulation of Heat shock factor by Hypoxia-inducible factor-1. *J Biol Chem* **281**: 38675-38681.

ACKNOWLEDGMENTS

I thank my advisor, Dr. Eric Johnson, for allowing me the freedom to design my own projects and experiments and for his seemingly endless supply of new scientific ideas. I also thank my family for fostering my curiosity and lifelong love of learning. Finally, I thank my wife Lisa for her love and support and for helping me to live each day to its fullest.

I dedicate this document to my father Valiant Richard Turnbull for the perfectionism and attention to detail I inherited from him. For this reason I owe my success in science and in life to him. Rest in peace Dad.

TABLE OF CONTENTS

Chapter Page

LIST OF FIGURES

Figure Page

Appendix

LIST OF TABLES

CHAPTER I

INTRODUCTION TO HYPOXIC GENE REGULATION AND NEXT GENERATION SEQUENCING

Background of hypoxic gene regulation

Molecular oxygen plays a multitude of essential roles in eukaryotic cellular physiology, perhaps most notably as the terminal electron acceptor in the electron transport chain of cellular respiration. Because of this critical role in cellular energy harvest, eukaryotic organisms have evolved several mechanisms to deal with situations where the supply of oxygen becomes scarce (hypoxia). One of the central hypoxic adaptations made by eukaryotic organisms is the differential regulation of specific sets of transcripts. By varying the amounts of transcripts for various genes, cells are able to alter quantities of assorted proteins, and by doing so, change their physiology in ways that allow them to better cope with hypoxia. This hypoxia-induced transcriptional modulation accomplished through the action of hypoxia-responsive transcription factors, proteins that are directly involved in regulating the quantities of transcripts that are produced from specific sets of genes.

The transcription factor with the best-characterized role in hypoxic gene regulation is Hypoxia Inducible Factor-1 (HIF-1) (1). HIF-1 is a heterodimeric transcription factor composed of two subunits known as HIF-1α and HIF-1β. HIF-1β is a protein that is constitutively present in many cells, and dimerizes with several other transcription factors other than HIF-1α in order to regulate transcription of genes involved processes as diverse as cellular responses to environmental toxins, to neural development (2). HIF-1β is absolutely essential for the function of HIF-1 as a hypoxia-responsive transcription factor, but plays little role in the regulation of its activation.

HIF-1α, on the other hand, is a protein that is tightly regulated by cellular oxygen levels, and this regulation is the key step in the regulation of HIF-1 activity. When oxygen is present in a cell at normal levels (normoxia), HIF-1α is hydroxylated at a proline residue by an enzyme known as HIF-1 Proline Hydroxylase (HPH). This hydroxylation reaction is dependent on the presence of molecular oxygen, and serves as the direct link between oxygen abundance and HIF-1α activity (3). When HIF-1α is proline hydroxylated, it is recognized by Von Hippel Lindau tumor suppressor protein (VHL), which facilitates the ubiquitination and rapid proteasomal degradation of the HIF-1α. This oxygen-dependent pathway prevents HIF-1α protein from ever being present at normal oxygen concentrations long enough to dimerize with HIF-1β and take part in transcriptional regulation. During hypoxia, however, HIF-1α is not degraded, dimerizes with HIF-1β, and the dimeric HIF-1 transcription factor activates the expression of its target genes.

When it is active in hypoxia, HIF-1 binds DNA sequence motifs with the core 5'-TRCGTG-3'. These elements are present, often in clusters, near genes that are regulated by HIF-1 under hypoxia. A number of genes have been identified as HIF-1 targets in mammalian and other model systems. HIF-1 is responsible for the transcriptional up-regulation of genes such as *erythropoietin (EPO),* and *Vascular endothelial growth factor (VEGF)* which increase oxygen delivery to hypoxic areas by stimulating red blood cell production, and the recruitment of blood vessels respectively in mammals(4). In the fruit fly *Drosophila melanogaster,* HIF-1 has been shown to regulate *HPH*, providing a feedback mechanism by which HIF-1 activity is attenuated during hypoxia (5). Nathan Baird and I showed that in *Drosophila*, HIF-1 directly regulates the transcription of *Heat shock factor* (HSF), a transcription factor that activates the transcription of heat shock protein genes (6). The full complement of HIF-1 regulated genes in *Drosophila* has not been exhaustively cataloged yet, however.

Another transcription factor that has been shown to regulate gene expression during hypoxia is the Forkhead transcription factor FOXO. FOXO activity is inhibited by Insulin signaling, causing FOXO to activate gene expression during starvation conditions. Mechanistically, FOXO is phosphorylated by the kinase AKT in response to Insulin or other growth factors. This phosphorylation causes the export of FOXO from the nucleus, thereby inhibiting FOXO-mediated transcriptional activation (7). Interestingly, elevated FOXO activity is linked to increased longevity in *Drosophila* and *Caenorhabditis elegans*, suggesting that the genes regulated by this transcription factor have significant protective functions for cells (7). Indeed, several genes involved in

reactive oxygen species detoxification have been described as FOXO targets, in addition to a number of genes involved in protecting cell from other stresses (8).

Recently, FOXO has been shown to activate gene expression in response to hypoxia in human cells (9). This study found that *FOXO3a*, one of the four FOXO transcription factors in humans, is transcriptionally activated by HIF-1 during hypoxia. This transcriptional up regulation contributes to the activation of FOXO-dependent gene expression during hypoxia. Interestingly, FOXO3a was found to activate transcription of *Cited2*, gene that is known to down-regulate HIF-1 activity, demonstrating that HIF-1 and FOXO3a regulate each other in a negative feedback loop.

Nuclear factor kappa-B (NFκB) is another transcription factor that has been shown to activate gene expression in response to hypoxia. NFκB has been most thoroughly characterized as a central transcriptional regulator of the inflammatory response in mammals (10). Under normal conditions, NFκB is bound by the repressor protein IκB, which masks the nuclear localization sequence (NLS), prevent nuclear accumulation of the transcription factor. NFκB can be activated by a number of stimuli, including bacterial antigens, proinflammatory cytokines, oxidative stress, and ultraviolet radiation. Upon activation, IκB is phosphorylated, ubiquitinated, and degraded, exposing the NLS of NFκB, which translocates in to the nucleus and activates transcription. Numerous NFκB target genes have been identified in multiple organisms, including those encoding inflammatory cytokines, chemokines, and cell adhesion molecules. In *Drosophila,* there are three NFκB proteins, Dorsal (Dl), Relish (Rel), and Dorsal-related immunity factor (Dif) (11). Dl has been extensively studied for its role in development.

Rel and Dif play key roles in the innate immune system of the fly, where they transcribe genes encoding anti-microbial peptides in response to bacterial and fungual infection.

Although numerous studies have shown that NFκB is activated by hypoxia, the mechanism by which this occurs is unclear (12) (13). There is evidence that hypoxia can induce the production of Nitric Oxide (NO) as well as other reactive oxygen species (ROS), and activation of NFκB by ROS has been well documented (14) (15). These observations seem to support the hypothesis that NFκB activation by hypoxia takes place because of a mechanism involving some sort of hypoxia-related change in the redox state of the cellular environment. Although we are not sure of the mechanism responsible, our lab has observed multiple targets of Rel, as well as Rel itself being transcriptionally up regulated by hypoxia in *Drosophila* (16).

Another stress-responsive transcription factor has been implicated in the hypoxia response is p53. This transcription factor is mainly known as a transcriptional activator of pro-apoptotic genes that is activated by DNA damage (17). A number of other stimuli can activate p53, including ultraviolet radiation, X-rays, low pH, and heat shock. In the absence of activating stimuli, p53 is ubiquitinated and targeted for degradation by the ubiquitin ligase MDM2. Hypoxia has been shown to activate p53 through direct binding and inhibition of MDM2 by HIF-1α (18). Other researchers have reported that ROS play a role in the hypoxic activation of p53 (19). The role of p53 in *Drosophila* hypoxic gene regulation has not been previously examined. Because *Drosophila* possesses a *p53* homologue, and ROS are known to be produced during hypoxia in the fly, it seems likely that p53 plays a role in hypoxic gene regulation in *Drosophila.*

Another hypoxia-responsive transcription factor that is likely to play a role in the hypoxia response of *Drosophila* is the Metal-responsive transcription factor-1 (MTF-1). MTF-1 is an evolutionarily-conserved transcription factor that possesses DNA binding zinc fingers which change conformation in response to fluctuations in cellular zinc concentration (20). MTF-1 activates the transcription of *Metallothionein* genes in response to increases in cytoplasmic metal ion levels. Metallothioneins are small, cysteine-rich proteins that bind zinc under physiological conditions. When other metal ions such as copper or cadmium enter the cytoplasm, Metallothioneins release their bound zinc and bind these more toxic ions with higher affinities. This mechanism allows MTF-1 to respond to a multitude of metals despite the fact that only zinc directly binds the transcription factor (21). Although the vast majority of work on MTF-1 has been directed toward understanding its role in cellular metal homeostasis, it has become clear that MTF-1 directs transcriptional changes in response to hypoxia as well. In human cells, the hypoxic transcriptional induction of Placenta growth factor (PIGF) was shown to be dependent on MTF-1 (22). Metallothionein genes have also been shown to be transcribed in response to hypoxia in an MTF-1-dependent manner (23). In *Drosophila*, our lab has observed transcriptional activation of *Metallothionein* genes during hypoxia, which is highly likely to require *MTF-1* (16).

Drosophila has been well established as an extremely powerful model system for uncovering fundamental new facets of genetics and molecular biology. Numerous cellular pathways that have key roles in human disease are also present in *Drosophila*, and in-depth molecular biological characterization of these pathways is much easier and more rapid in the fly due to its short generation time and widely available genetic tools.

Each of the five hypoxia-responsive transcription factors that I described in the preceding pages is present in *Drosophila*. In this dissertation, I describe my work on understanding the transcriptional response to hypoxia using the *Drosophila* model system. I examined hypoxia-responsive gene expression in five different fly lines, deficient in *HIF-1, FOXO, NFκB, p53,* and *MTF-1*. By combining this analysis with bioinformatics, I was able to determine, to a large extent, the role of each transcription factor in the broader transcriptional hypoxia response. My work represents the first dissection of the transcriptional hypoxia response to this level of detail. This would not have been possible without use of the *Drosophila* model system.

Background of genomic regional enrichment for sequencing

It could be said that the blueprint for an organism lies in the sequence of its genome. Because the genomic sequence of any living thing contains so much useful information about the biology of that organism, a great deal of effort has been devoted to genome sequencing projects. The genome sequences produced by these projects make molecular biological studies enormously easier than they would be in the absence of reference genome sequences for the organisms being studied.

The bulk of existing genomic sequence data has been produced using variations of the chain-terminator method of DNA sequencing developed by Frederick Sanger and colleagues in the 1970's (24). In this method, DNA polymerase synthesizes a new strand of DNA from a specific primer that has been annealed to the DNA template that is to be sequenced. This synthesis takes place in the presence of a small concentration of dideoxynucleotides, which, when incorporated in to the newly synthesized strand,

prevent DNA polymerase from adding additional nucleotides and thus terminate the synthesis of the new chain of nucleotides. This results in the synthesis of new DNA strands from the sequencing primers that are a multitude of lengths. In modern Sanger sequencing, the dideoxy terminator nucleotides also incorporate specific fluorophore moieties for each of the four dideoxynucleotides in the reaction. When the DNA synthesis is complete, the mixture of product strands is separated by size using electrophoresis to a resolution that allows the researcher to discern size differences of one nucleotide. By observing the size of each fragment and taking note of the fluorescent color of the chain-terminator nucleotide that was incorporated, the researcher can deduce the sequence of the newly synthesized DNA strand beginning at the 3' end of the sequencing primer.

The reads produced by Sanger sequencing are typically less than one kilobase (kb) in length. This read length is 3,000,000 times smaller than the length of the human genome, for example, making the task of sequencing entire genomes using the Sanger approach laborious and costly. The desire to sequence new genomes more quickly as well as a need to determine sequence polymorphisms at the root of genetic diseases has led to the development of several types next generation DNA sequencing (NGS) technology. These NGS approaches all are based on the concept of sequencing massive numbers of random DNA fragments in parallel. Each sequencing read from a NGS run is much shorter than those produced in a Sanger sequencing run; the advantage that NGS provides lies in the number of reads produced by these approaches. For example, the individual sequencing reads produced by Illumina Genome Analyzer II NGS instrument

are 50 nucleotides or less in length, however, this instrument produces roughly 96,000,000 of these reads which results in 4.8 gigabases of raw sequence information.

Due to sequencing errors and the necessity of significant overlap between individual reads for assembly into a long continuous sequence, NGS instruments can still not sequence entire genomes of higher eukaryotes in single runs. In many cases, researchers are only interested in sequencing portions of a genome, such as when identifying disease related single nucleotide polymorphisms (SNPs) in clinical samples, or when attempting to identify the SNP responsible for an interesting phenotype in a mutant identified in a genetic screen. NGS instruments, however, do not sequence targeted genomic regions; random DNA fragments serve as the sequencing template resulting in reads that are scattered throughout the genome. Sanger sequencing allows researchers to select the region they would like to sequence based on the location of the sequencing primer, but sequencing large regions requires the design of numerous primers that each must be run in a separate sequencing reaction making the targeted sequencing of large regions with Sanger technology both slow and expensive. For these reasons, several groups are pursuing methods for selecting large genomic regions for sequencing by NGS.

Two independent groups published methods for targeted sequencing of large genomic regions by NGS last year (25, 26). Both of these papers describe essentially the same protocol in which custom DNA microarrays are designed and constructed to contain oligonucleotide sequences that are homologous to a large genomic region of interest. Genomic DNA is randomly sheared and hybridized to the custom microarray, and the sequences that are not homologous to those represented on the array are washed away.

The genomic fragments that hybridized to the array are then eluted by denaturation, amplified, and sequenced by NGS. This approach has proven to be an effective method of isolating and sequencing specific large genomic regions.

I have developed an alternative method to the custom microarray based approach for capturing large genomic regions for sequencing by NGS. My method uses fosmid or bacterial artificial chromosome (BAC) DNA that is homologous to the genomic region of interest in place of the custom microarrays that are used in the previously published protocols. My method is significantly faster, and can be completed for a small fraction of the cost of microarray-based methods. Furthermore, no complete reference genome sequence for the target region is required by my technique. The low cost and simplicity of my technique will make current NGS technology an effective means of sequencing large genomic regions for more than only the most well funded research groups in the world.

P.D. Etter contributed to the research described in Chapter II as a second author. N.A Baird was the first author of Chapter III. I.T. Helenius and T. Krupinski were co-first authors and Y. Gruenbaum was the third author of Chapter IV.

Bridge to Chapter II

In the previous chapter I described what is known about the hypoxia-responsive transcriptional regulatory activities of HIF-1, FOXO, NFκB, p53, and MTF-1. In Chapter II, I will report the identities of numerous genes that are regulated by each transcription factor during hypoxia in *Drosophila melanogaster.*

CHAPTER II

GENETIC DISSECTION OF THE TRANSCRIPTIONAL HYPOXIA RESPONSE IN *DROSOPHILA MELANOGASTER*

P.D. Etter contributed to this work by performing the genetic crosses and microarray experiments for two of the six genetic strains used. I conducted the remainder of the experiments as well as the data analysis and writing.

Oxygen is required by all multicellular organisms for survival. When animals are deprived of oxygen, they undergo a complex series of behaviorial, developmental, physiological and molecular changes in order to survive the challenge. Hypoxia is also encountered by cells in tissues affected by heart attack, stroke, wounding, as well as within poorly vascularized tumors. Hypoxic tumors are often resistant to treatment, and indicate a poor prognosis for cancer patients (27). Due to the medical importance of hypoxia, a great deal of research has been devoted to understanding the mechanisms cells utilize to survive this stress.

One mechanism widely utilized by organisms to cope with oxygen deprivation involves the modulation of gene expression in response to hypoxia. The transcription factor HIF-1 has been well characterized as a regulator of hypoxia-responsive gene

expression (1). HIF-1 is a heterodimeric transcription factor composed of an α and a β subunit. HIF-1α is rapidly ubiquitinated and degraded in the presence of oxygen, but during periods of hypoxia the protein dimerizes with HIF-1β, which is constitutively expressed, to form the active HIF1 transcription factor complex. HIF-1 binds genomic regulatory elements known as hypoxia response elements (HREs), where it is transactivated and facilitates the transcriptional activation of genes that help cells survive hypoxia by either decreasing their demand for oxygen by shifting to glycolytic metabolism, increasing the supply of oxygen by recruiting blood vessels to the hypoxic area, or by stimulating the production of red blood cells (1).

In addition to HIF-1, other transcription factors are known to take part in regulating hypoxic gene expression. Nuclear factor kappa-B (NFκB) transcription factors play a large part in regulating gene expression in response to inflammatory stimuli and are also known to be activated by hypoxia (12) (13). Another transcription factor that has been shown to regulate gene expression in response to hypoxia is p53, which is a key regulator of genes that are responsible for the induction of apoptosis (28). The FOXO family of Forkhead transcription factors regulate gene expression in response to a multitude of stresses, and have recently been shown to be involved in regulating the transcriptional response to hypoxia in human cells(9). Although primarily characterized as a regulator of genes involved in the cellular response to heavy metal stress, the metal response element (MRE) binding transcription factor (MTF-1) has also been shown to respond to nitric oxide as well as hypoxia (29) (23). While NFκB, p53, FOXO, and

MTF-1 are all known to be hypoxia-responsive transcription factors, the comprehensive set of genes regulated by each during hypoxia have yet to be determined.

Much of what is currently known in the field of genetics was gleaned from the study of the fruit fly *Drosophila melanogaster*. *Drosophila* has also proven to be an effective model system for the study of hypoxia. The *Drosophila* proteins Similar and Tango have been identified as functional homologues of mammalian HIF-1α and HIF-1β (30, 31). Functional homologues of the hypoxia-responsive transcription factors NFκB, p53, FOXO, and MTF-1 are also present in *Drosophila*. Previously, our lab used microarrays to identify *Drosophila* genes that are transcribed in response to hypoxia (16). In the present study, we used available mutant *Drosophila* strains deficient in HIF-1 ($sima^{7607}$), NFκB (rel^{e20}), p53 ($p53^{5A-1-4}$), FOXO ($foxo^{21}/foxo^{25}$), and MTF-1 ($mtf\text{-}1^{140\text{-}1R}$), to identify hypoxia-responsive transcripts that are regulated by each respective transcription factor.

Materials and Methods

Drosophila strains. In order to minimize differences in gene expression due to variations in the genetic backgrounds of the strains that were studied, both the wild type Oregon R control strain and each mutant were crossed to a strain bearing visible markers on each chromosome (*yw;Sp/cCyO;dDp/TM3-Sb)*. The genotype of the wild type control strain was *yw;Sp/CyO;+*. The genotypes of the mutant strains studied were as follows: $yw;Sp/CyO;sima^{7607}$, $yw;Sp/CyO;foxo^{21}/foxo^{25}$, $yw;Sp/CyO;p53^{5A-1-4}$, $yw;Sp/CyO;rel^{e20}$, and $yw;Sp/CyO/mtf\text{-}1^{140\text{-}1R}$.

Hypoxia treatment. Twenty male and female adult flies between the ages of 1 and 5 days post-eclosion were collected from each genotype and placed in separate vials containing standard *Drosophila* medium for each hypoxia experiment. Six replicate populations were collected for each genotype. After a 24-hour recovery period following counting, three of the vials for the wild type strain and each mutant were placed in a sealed chamber at room temperature that was then flushed with a mixture of 0.5% O_2 and 99.5% N_2 (hypoxia). The three other vials for each respective genotype were placed in an identical chamber containing normal atmospheric oxygen concentrations (normoxia). The flies were incubated in the hypoxia and normoxia chambers for six hours, following which they were rapidly removed and frozen in liquid N_2.

RNA extraction and DNA microarray experiments. Following either hypoxia or normoxia treatment, frozen flies were homogenized in TRIzol reagent and RNA was extracted according to the manufacturer's protocol (Invitrogen). For each strain, 20 μg of RNA from each normoxia and hypoxia treatment were labeled for microarray hybridization using the SuperScript Direct cDNA Labeling System (Invitrogen), incorporating either Cyanine 3 (normoxia) or Cyanine 5 (hypoxia) conjugated dUTP (Perkin Elmer). In each strain, gene expression during hypoxia was assayed by combining labeled normoxia and hypoxia cDNA, and hybridizing the samples to DNA microarrays containing 16,416 oligonucleotides from the INDAC set representing the *D. melanogaster* transcriptome (Illumina). Three microarrays were hybridized for each mutant, representing three independent biological repeats. Microarrays were scanned and analyzed using Gene Pix Pro 6.0 software (Molecular Devices).

Microarray Data Analysis. In order to identify the complete set of hypoxia-modulated transcripts, we identified transcripts in wild type flies that increased or decreased greater than 1.6 fold during hypoxia (average of 3 microarray data sets). We then examined the expression level of this set of transcripts in each mutant strain. In order to identify genes that were differentially regulated during hypoxia in each mutant strain, we used BAMarray^{TM} 2.0 software, which utilizes Bayesian ANOVA analysis to identify significant differences in transcript levels between multiple microarray data sets (32). Conserved binding sites for each transcription factor were identified using our own software (http://genomix.uoregon.edu/~eric-johnson/cgi-bin/GAS.pl). The motifs used for each transcription factor binding site search are as follows: Sima - TACGTG; dFOXO - RTAAACAA; Rel - GGGAHNYMY; p53 - RRRCWWGYYY; MTF-1 - TGCRCNC. Groups of 2 or more binding sites within 2 kb of an open reading frame that are conserved in *D. melanogaster* as well as at least three other *Drosophilid* genomes were considered likely to be functional binding sites for the transcription factor being queried.

Results

Hypoxia-induced changes in gene expression—DNA microarrays were used to compare transcriptional profiles of adult *Drosophila melanogaster* flies that had been exposed to hypoxia to those of flies that were kept at atmospheric oxygen concentrations. Upon treatment with hypoxia, 435 transcripts were either up- or down-regulated greater than 1.6 fold (3.05% of the transcripts represented on the array). These results are in agreement with the set of transcripts that we previously identified as being induced by

hypoxia (16). In order to identify transcription factors involved in the regulation of the identified hypoxia modulated transcripts, we examined hypoxia-responsive gene expression in mutant strains deficient in *Sima, dFOXO, NFκB, p53*, and *MTF-1*.

Hypoxia-responsive gene regulation in mutant strains-- In order to minimize differences among the mutants due to variation in their genetic backgrounds, we performed a series of crosses to make each mutant genetically identical to the wild-type strain, with the exception of the chromosome containing each respective mutation. We then exposed each mutant strain to the same hypoxia treatment as the wild type flies and identified transcripts that were either induced or repressed by hypoxia using microarrays. Baesian ANOVA analysis was then used to identify transcripts that were differentially regulated under hypoxia between wild type flies, and each mutant strain (Figure 1) (32).

Of the 435 transcripts that were induced or repressed 1.6 fold or greater during hypoxia in wild type flies, 190 were identified as significantly different in any one of the mutant strains by Bayesian ANOVA analysis. We analyzed the expression or each of these 190 genes by hierarchical clustering (Figure 2). Interestingly, d*FOXO* mutants exhibit the greatest difference in hypoxia-induced gene regulation when compared to wild type flies by hierarchical clustering. *Sima* mutants exhibit the second largest difference in hypoxic gene regulation from wild type flies, while *p53, rel,* and *MTF-1* exhibit patterns in gene regulation that are more similar to wild type.

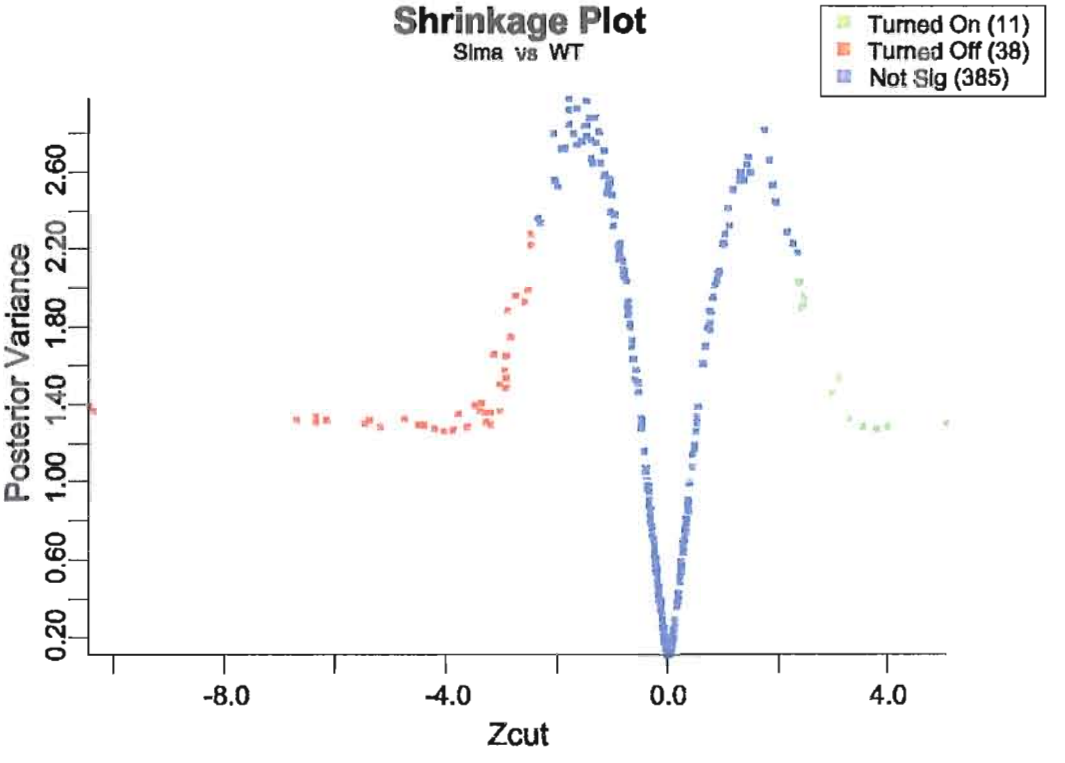

Figure 1. Example data plot from BAMarray™ Bayseian ANOVA data analysis comparing the expression of 435 hypoxia-regulated transcripts in *sima-* and *WT* flies. Genes are classified as significantly differentially expressed between two data sets when their Zcut values are large, and their posterior variances are close to 1. BAMarray™ automates the selection of such genes using a rule based on the specific data set. For details of BAMarray™ statistics, please see {Ishwaran et al., 2006, BMC Bioinformatics, 7, 59}.

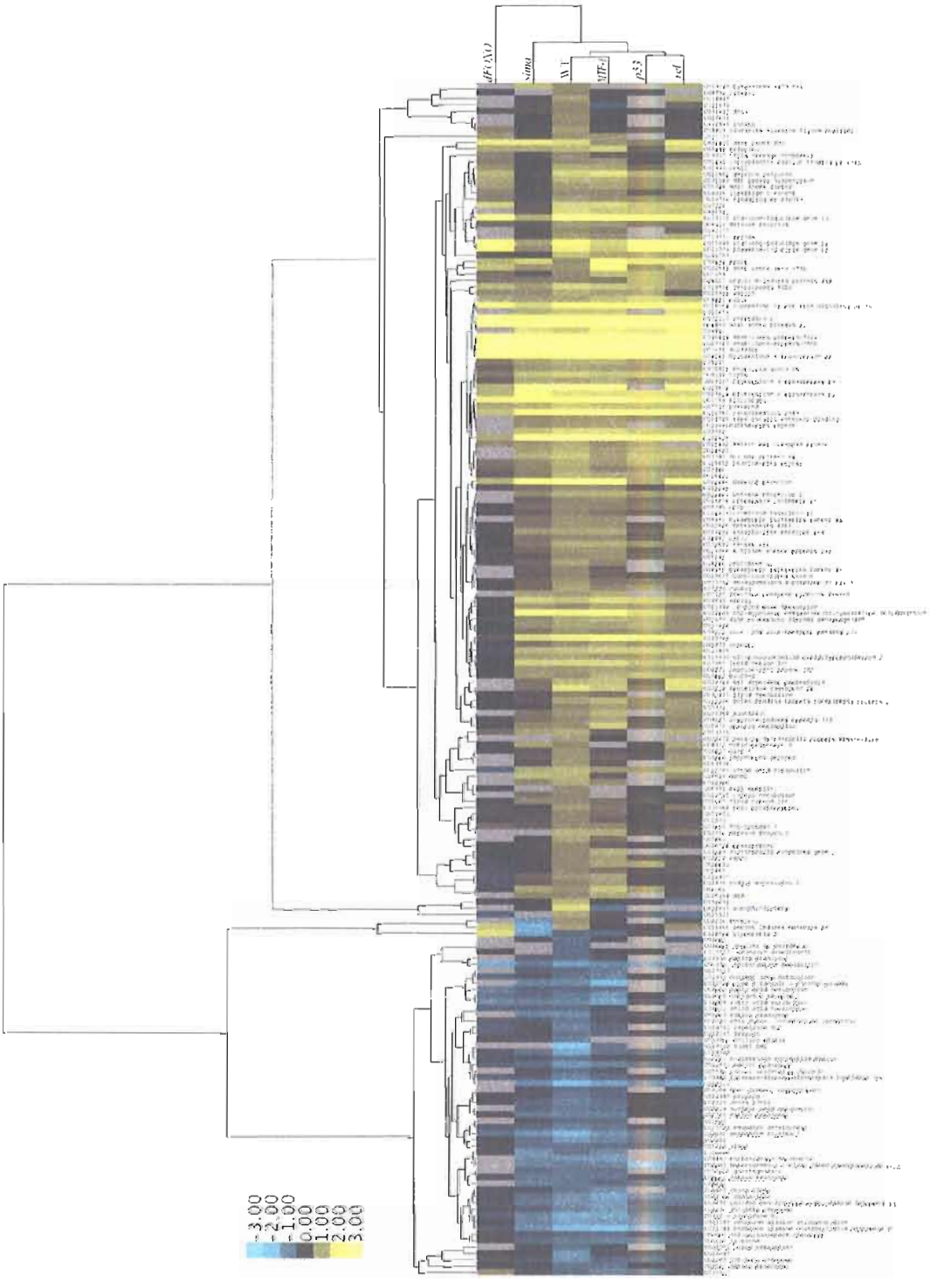

Figure 2. Hierarchical clustering of hypoxia modulated transcripts with significantly perturbed expression levels in at least one mutant strain. Rows represent the average expression levels of transcripts from 3 biological replicates for the strain indicated in each column. During hypoxia, *dFOXO* mutants exhibit the greatest difference from wild type flies, followed by *sima* mutants.

In order to refine the lists of target genes to include only direct transcriptional targets of each transcription factor under hypoxia, and to eliminate genes indirectly affected by the loss of that factor, we used a bioinformatic approach (Figure 3). Genes were considered strong candidate targets of a given transcription factor under hypoxic conditions if they showed significantly altered expression levels in that mutant under hypoxia and also contained two or more conserved binding sites for the affected transcription factor within two kilobases of the open reading frame. Based on these criteria, we identified 47 hypoxia modulated target genes for dFOXO, 24 targets of Sima, 16 targets of Relish, 14 targets of p53, and 14 MTF-1 targets (Table 1). These numbers are in accordance with the differences in hypoxic transcriptional modulation between each mutant strain and wild type based on hierarchical clustering, with FOXO being required for the hypoxic modulation of the greatest number of transcripts, followed by Sima, Rel, p53, and MTF-1 (Figure 2).

Table 1. Hypoxia modulated transcripts with significantly altered hypoxia expression levels in mutant strains

Transcript	Fold hypoxic induction in WT	Fold hypoxic induction in mutant	Conserved binding sites
dFOXO-dependent transcripts			
CG18466 NAD-dependent methylenetetrahydrofolate dehydrogenase	3.94	1.06	4
CG10383	3.66	1.25	5
CG7219 Proteinase inhibitor I4	3.36	0.00	2
CG5966 lipid metabolism	3.01	1.00	2
CG8709 lipid metabolism	2.93	1.42	6
CG7850 puckered	2.85	1.93	8
CG5953	2.77	0.00	8

CG3090 Sox box protein 14	2.66	0.00	2
CG13868	2.39	0.79	7
CG3705 astray	2.39	1.05	2
CG14801 nucleic acid metabolism	2.22	0.00	8
CG32369 carbohydrate metabolism	2.22	0.00	6
CG15423	2.22	1.24	2
CG11796 amino acid catabolism	2.20	0.69	3
CG7554 comm2	2.17	0.00	2
CG5295	2.13	1.41	3
CG12489 Defense repressor 1	2.04	0.00	10
CG1600 Zinc-containing alcohol dehydrogenase superfamily	2.01	1.15	6
CG31811 centaurin gamma 1A	1.96	1.29	5
CG5467	1.93	0.00	3
CG5246 proteolysis Peptidase S1	1.93	1.13	2
CG16926	1.91	0.91	2
CG12358 polyA-binding protein interacting protein 2	1.89	1.03	3
CG32972 cell adhesion	1.84	0.00	4
CG10580 fringe	1.82	0.00	6
CG7525 Tie-like receptor	1.78	0.00	2
CG15162 Misexpression suppressor of ras 3	1.73	0.96	3
CG12845 Tetraspanin 42Ef	1.73	1.07	2
CG8222 PDGF- and VEGF-receptor related Pvr	1.72	1.03	2
CG31319 RhoGAP88C	1.71	0.00	3
CG3234 timeless	1.71	0.00	2
CG5248 locomotion defects	1.69	0.00	3
CG13388 A kinase anchor protein 200	1.67	1.13	2
CG1921 sprouty	1.66	1.04	3
CG5461 bunched	1.64	1.00	19
CG4993 PRL-1	1.59	1.03	5
CG8095 scab	1.59	1.06	2
CG8127 Ecdysone-induced protein 75B	1.57	1.05	24
CG14401	1.57	0.83	3
CG10637 Numb-associated kinase	1.53	0.00	3
CG7210 kelch	1.53	0.92	2
CG17278 Proteinase inhibitor 11	1.52	0.00	2
CG8098 Picot	0.63	0.93	4
CG13607	0.62	1.06	2
CG7720 cation transport	0.54	1.01	7
CG12602 cation transport	0.42	0.74	2

Sima-depenndent transcripts

CG31449 Heat-shock-protein-70Ba	4.91	3.89	2
CG10160 Ecdysone-inducible gene L3	3.06	1.09	2
CG15009 Ecdysone-inducible gene L2	2.13	0.92	6
CG7224	1.60	0.30	3
CG11652 DPH2 protein 68D2	1.56	0.15	2
CG31769	1.29	-0.07	2

CG31543 HIF prolyl hydroxylase	1.16	-0.02	9
CG1333 Ero1L	1.05	-0.04	2
CG5467	0.95	0.10	4
CG6246 nubbin	0.95	0.41	4
CG12358 polyA-binding protein interacting protein 2	0.92	0.27	5
CG32972 Beta-Ig-H3/fasciclin Protein kinase-like 35A1	0.88	0.00	5
CG5748 Heat shock factor	0.86	0.08	3
CG30069 cell cycle	0.85	-0.05	3
CG10746 fledgling of Klp38B	0.84	-0.22	4
CG8913 oxygen and reactive oxygen species metabolism	0.83	0.22	3
CG3234 timeless	0.77	-1.20	2
CG9078 infertile crescent	0.66	0.11	2
CG10827 Alkaline phosphatase	-0.66	0.00	2
CG12385 Peptidase S1	-0.70	-0.17	2
CG13997	-1.21	-0.06	2
CG12602 cation transport	-1.24	-0.63	3
CG10129 nudel	-1.97	0.00	3

Relish-dependent transcripts

CG32130 apoptosis proteolysis Peptidase S1	4.72	7.00	5
CG18466 NAD-dependent methylenetetrahydrofolate dehydrogenase	3.94	1.75	4
CG3896 defense response	2.11	1.41	2
CG11992 Relish	2.03	1.00	4
CG5467	1.93	1.08	3
CG32972 cell adhesion	1.84	1.00	3
CG17631	1.64	1.06	2
CG10248 Cytochrome P450-6a8	1.53	2.00	6
CG1701	0.64	0.94	3
CG8098 Picot	0.63	0.98	2
CG10827	0.63	1.00	2
CG12387 Trypsin	0.58	0.88	2
CG17876 Amylase distal	0.55	1.00	4
CG8083 cation transport	0.48	0.70	2
CG12602 cation transport	0.42	0.67	2

MTF-1-dependent transcripts

CG4463 Heat shock protein 23	5.13	10.80	3
CG5550 defense response	5.10	8.30	2
CG14847	1.84	0.95	3
CG4919 Glutamate-cysteine ligase modifier	1.82	1.00	2
CG1399 Leucine-rich repeat	1.77	1.88	8
CG3234 timeless	1.71	1.13	5
CG32041 Heat shock gene 67Bb	1.69	4.63	5
CG9568	1.67	2.63	2
CG4312 Metallothionein B	1.59	0.00	5

CG5059	1.56	2.35	4
CG10725 chitin metabolism	1.53	0.00	2
CG10827 Alkaline phosphatase	0.63	0.94	4
CG1941	0.60	0.99	2
CG17876 Amylase distal Amy-d	0.55	0.00	3

_p53_-dependent transcripts

CG8127 Ecdysone-induced protein 75B	1.53	2.27	12
CG30069 cell proliferation	1.80	0.94	8
CG7720 cation transport	0.54	0.91	5
CG10827 mesoderm development	0.63	1.03	4
CG32972 cell adhesion	1.84	0.00	3
CG10580 fringe	1.82	0.00	3
CG13503 actin filament organization	1.73	0.00	3
CG31319 RhoGAP88C	1.71	0.00	3
CG12602 cation transport	0.42	0.63	3
CG5246 proteolysis Peptidase S1	1.93	0.00	2
CG18402 Insulin-like receptor InR	1.91	1.30	2
CG6437 GlcT-1	1.68	1.11	2
CG1941	0.60	0.00	2
CG10129 nudel Toll signaling pathway	0.26	0.00	2

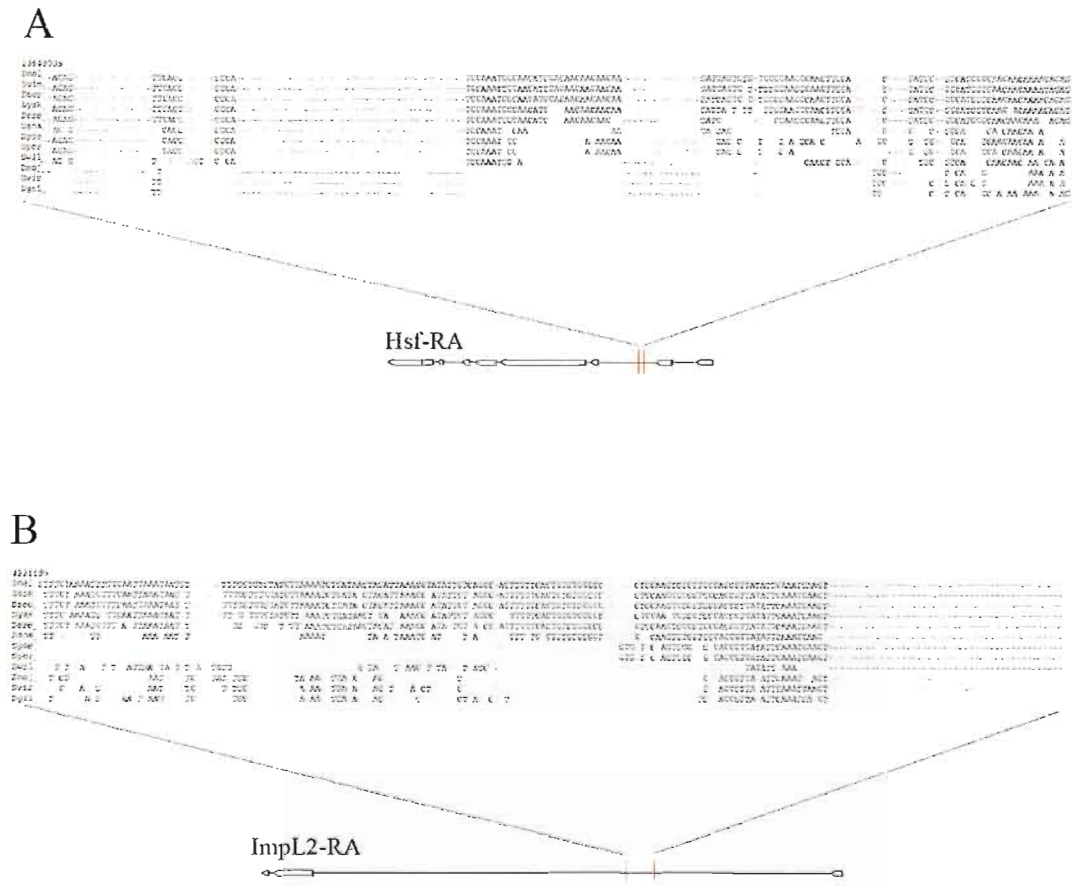

Figure 3. Examples of computationally identified conserved binding sites for putative hypoxia-responsive transcription factor targets. Transcripts identified as differentially expressed during hypoxia in *sima* mutants contained both known Sima targets such as *Heat shock factor* (A), and transcripts that have previously been uncharacterized as targets of Sima, such as *Imp-L2* (B). Both transcripts contain Sima binding sites within introns that are conserved in multiple *Drosophila* species.

Discussion

The transcriptional regulation of genes during hypoxia has been examined in many model systems. However, the exact roles of many of the transcription factors known to be involved in the hypoxic response and how they regulate gene expression during hypoxia have not been comprehensively determined until now. We identified 435 transcripts that are either induced or repressed greater than 1.6 fold by hypoxia in wild

type *D. melanogaster*. Of these genes, 190 (43.7%) are significantly differentially regulated during hypoxia in flies that are deficient in at least one of the transcription factors we examined. In order to separate genuine targets of the hypoxia-responsive transcription factors from transcripts that change in abundance due to indirect effects, we computationally identified conserved transcription factor binding sites near putative target genes identified in each mutant strain. Following this analysis, we identified 88 transcripts as being regulated by at least one of the transcription factors we examined.

Interestingly, the vast majority of hypoxia-modulated transcripts we were able to assign to a particular transcription factor were those that were up-regulated by hypoxia. Relish was the only transcription factor out of the five we studied that seems to play a substantial role in transcriptional repression during hypoxia; 43.75% (7/16) of the genes regulated by Rel during hypoxia are down-regulated by the stress in wild type flies. Interestingly, in the absence of *Rel*, several hypoxia modulated transcripts are more highly transcribed, supporting the potential role of Rel as a hypoxia-responsive transcriptional repressor. Several *MTF-1*-dependent transcripts are more highly induced by hypoxia in the transcription factor's absence, suggesting that MTF-1 functions as a repressor as well. Each of the other transcription factors appear to function more as transcriptional activators during hypoxia; of the dFOXO regulated genes, 91.49% were up-regulated, 79.17% of Sima dependent genes were up-regulated, and 64.3% of p53 dependent genes were up-regulated.

To our surprise, dFOXO appears to regulate the expression of the greatest number of hypoxia-modulated transcripts of all the transcription factors we examined, including Sima, the homologue of HIF-1α, which is widely considered to be the master regulator of

hypoxia-induced gene expression. While this may be partially due to the relative strength of the alleles we used, it is still an unexpected result. This study constitutes the first characterization of dFOXO as a major regulator of hypoxia-induced gene expression. It will be interesting to determine the extent to which FOXO transcription factors function during hypoxia in other organisms. In future experiments, we plan to examine dFOXO mutants that have been raised at non-lethal levels of hypoxia and determine whether they exhibit observable developmental or reproductive phenotypes. These experiments will further validate our identification of dFOXO as a major regulator of gene expression during hypoxia.

Sima, the *Drosophila* homologue of HIF-1α, has previously been characterized as a regulator of hypoxic gene expression (31). Our experiments have shown that Sima does indeed regulate a large number of genes during hypoxia. The set of Sima-regulated transcripts that we identified includes genes such as *Heat shock factor (Hsf)* and *HIF prolyl hydroxylase* (*HPH)* , which have been previously characterized as direct targets of Sima (Table 1)(5, 6). We also identified several transcripts that have never been previously described as Sima targets. One of these encodes Imaginal morphogenesis protein-Late 2 (Imp-L2), a protein that has recently been characterized as a negative regulator of the insulin signaling pathway in *Drosophila* (33). This is an intriguing result because it may prove to be a link between the activities Sima and dFOXO during hypoxia. Because Imp-L2 inhibits the activity of Insulin-like peptide, which participates in a pathway that in turn inhibits the activity of dFOXO, the Sima-dependent up-regulation of Imp-L2 may result in the up-regulation of dFOXO activity during hypoxia

(Figure 4). We are currently conducting experiments to explore this regulatory link, as well as a possible role of Imp-L2 as a hypoxia-induced inhibitor of growth.

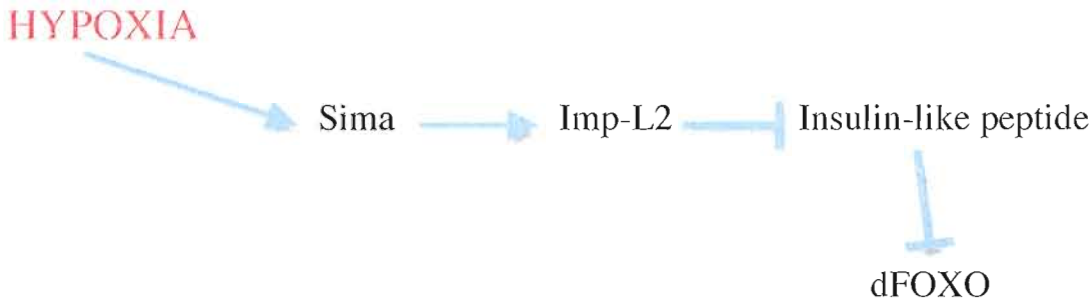

Figure 4. Schematic representation of a potential regulatory mechanism by which Sima likely contributes to the activation of dFOXO during hypoxia through transcriptional up-regulation of *Imp-L2*.

There are several other interesting results from our analysis. Relish, a transcription factor that has been previously identified as a regulator of the transcriptional response to Gram-negative bacterial infection, also regulates the expression of several genes in response to hypoxia. This may serve to sensitize the innate immune system of flies during hypoxia, a condition that likely coincides with areas containing large amounts of microbes when encountered by flies in their natural environment. We have frequently observed stochastic transcriptional activation of antimicrobial peptide genes in wild type flies exposed to hypoxia (unpublished data). This may be due to hyper-sensitization of the fly's innate immune system by hypoxic activation of Relish.

MTF-1 and p53 have both been implicated in hypoxia-induced gene regulation in mammalian systems (34, 35). Our data indicates that these transcription factors are active under hypoxia in *Drosophila* as well. It has been previously demonstrated that MTF-1 activates the transcription of *Metallothionein* genes in response to hypoxia (23),

and we have shown that this also occurs in *Drosophila* in the case of *Metallothionein B*. We have also identified several other hypoxia-induced targets of MTF-1. The group of p53-dependent hypoxia modulated transcripts we identified contains several interesting genes. We identified *Fringe*, a regulator of the Notch signaling pathway, as a target of p53 during hypoxia. Activation of the Notch pathway during hypoxia has been observed in other organisms (36). It will be interesting to determine whether the Notch pathway is activated by hypoxia in *Drosophila* as well.

In order to survive hypoxic stress, organisms undergo a complex series of both behavioral and physiological adaptations, including the transcriptional activation and repression of sets of genes. In addition, cells within dense and rapidly growing tumors frequently encounter hypoxia, and must alter their transcriptomes in order to survive. For these reasons, understanding the mechanisms by which transcription is altered during hypoxia not only broadens our understanding of how organisms endure physiological stress, but also provides information that may be useful in designing strategies to prevent cells within hypoxic tumors from surviving and proliferating. Our group and others have previously identified transcripts that are induced and repressed by hypoxia in *Drosophila* and other organisms. In the present study, we illuminated the roles of five different hypoxia-responsive transcription factors in the broader transcriptional hypoxia response. This represents the most in depth dissection of the transcriptional hypoxia response to date. We have shown that dFOXO regulates a surprisingly large number of transcripts during hypoxia, and have identified several interesting targets of Sima, Rel, MTF-1, and p53 that likely play a multitude of important functional roles during hypoxia, and warrant further in-depth investigation.

Bridge to Chapter III

In the previous chapter, I described experiments that identified genes that are regulated by HIF-1, FOXO, NFκB, p53, and MTF-1 during hypoxia. In Chapter III, I report data from a published paper, of which I was the second author, that examined one HIF-1 target gene in detail. We show how this regulation constitutes cross-talk between two stress response pathways, and that it is important for viability under hypoxia.

CHAPTER III

HEAT SHOCK PATHWAY IS ACTIVATED BY THE DIRECT REGULATION OF HEAT SHOCK FACTOR BY HIF-1 DURING HYPOXIA

I performed the chromatin IP experiments described in this paper, which showed that HIF-1 directly binds the regulatory region of the *HSF* gene. I also conducted DNA microarray experiments prior to the research described that allowed us to identify *HSF* as a likely *HIF-1*target.

In order to endure oxygen deprivation, most eukaryotes utilize a conserved set of cellular adaptations (37). Many of these changes are brought about by the activation of the transcription factor HIF-1, a heterodimeric complex composed of HIF-1α and HIF-1β subunits. When this complex is formed it binds to specific DNA enhancer sequences and regulates the activity of target genes. Both HIF-1α and HIF-1β are constitutively expressed in normal oxygen conditions (normoxia), but HIF-1α protein is quickly degraded before dimerization can occur with HIF-1β (3). Normoxic HIF-1α degradation

is mediated by a series of hydroxylations and ubiquitinations, which tag HIF-1α for disposal through the proteasome (38) (39) (40) ()41

The HIF-1 complex transcriptionally regulates a wide array of genes involved in anaerobic metabolism, growth, proliferation, angiogenesis, and cell death (42) (43). This multifaceted control of cellular and organismal physiological pathways is exploited by solid tumors through the natural hypoxic environment caused by rapid growth or genetic alterations which stabilize HIF-1α (44). Overexpression or activation of HIF-1α is often seen in a wide array of cancers and is correlated with patient survival (45), and studies have shown that targeting the HIF-1 pathway is a promising means of cancer therapy (46). Thus, HIF-1 is a central regulator of normal and pathological changes in response to low oxygen.

While many genes that are up-regulated during hypoxia are known to be regulated by HIF-1, there are also diverse sets of genes up-regulated that have not been linked to the actions of HIF-1. Among these are the highly conserved heat shock proteins (Hsps) that are highly up-regulated during hypoxia but have not been linked to HIF-1 regulation (47). Hsps are known to act as cellular chaperones for proteins that are misfolded by cellular stresses (48). Heat shock factor (Hsf) was one of the first studied transcription factors and its activation by stresses that promote the unfolding of proteins has been well characterized. When cells are unstressed Hsf is in a monomeric state, but cellular stress induces trimerization of the protein(49) (50). The trimeric form of Hsf activates transcription of downstream genes, such as *Hsps* (51) (52). However, this study identifies a novel mode of regulation of heat shock pathway activity during hypoxia through a HIF-1-dependent increase in Hsf transcript levels. This up-regulation of *Hsf* is

necessary for the full increase of Hsp transcripts normally observed during hypoxia and also during reoxygenation. These findings establish a novel regulatory link between two stress pathways previously thought to be independent in responding to hypoxia.

Results

Hsf transcript levels increase during hypoxia in a HIF-1α-dependent manner

Drosophila melanogaster Kc_{167} cells were treated with GFP control double-stranded RNA (dsRNA) or dsRNA directed to eliminate transcripts of the *Drosophila* HIF-1α homologue, *similar* (31) (53), through RNAi. After exposure of the treated cells to normoxic or hypoxic conditions, total RNA was isolated for semi-quantitative reverse transcription-PCR in order to characterize the transcript levels of HIF-1α, Hsf, and Actin5c as a control (Fig. 1A). Interestingly, we found that transcript levels of Hsf increased during hypoxia, and that this up-regulation was HIF-1α-dependent. Cells lacking HIF-1α due to RNAi did not display a hypoxic increase in Hsf, instead maintaining Hsf levels more similar to control normoxic cells. Real-time PCR was then used to more accurately characterize these results (Fig. 1B) and further corroborated that Hsf transcripts increase under hypoxic conditions in a HIF-1α-dependent manner. As an additional control we repeated the RNAi with an alternate dsRNA sequence targeting another area of HIF-1α, which also showed a HIF-1α-dependent hypoxic increase of Hsf (Fig. 1C). This control experiment confirms our results were not due to off-target effects of the original RNAi.

The increase in Hsf transcript levels during hypoxia is directly regulated by HIF-1α

The DNA recognition element to which HIF-1 binds during hypoxia contains a core 5'-RCGTG sequence (54) We had identified multiple instances of a related motif, 5'-TACGTGC, in the intron of the known HIF-1 target gene (55) HIF-1 *prolyl hydroxylase* (PHD), and searched for this motif in the *Hsf* gene region. We identified two of these putative hypoxia response elements (HREs) in close proximity to one another in the second intron of *Hsf*. The two sites were 923 and 992 base pairs (bps) downstream from the transcriptional start site of *Hsf* respectively. When this genomic region was aligned (56) with seven other *Drosophila* species these potential HREs were perfectly conserved (Fig. 2A). The sequence conservation of the two HRE motifs strongly suggests that there is evolutionary pressure to maintain these specific sequences.

We next tested if these conserved HRE motifs had a regulatory function during hypoxia. A portion of the second intron of *Hsf* containing the potential HREs was cloned upstream of a minimal promoter driving GFP in the Green H Pelican reporter vector (57). This reporter construct was then transfected into the Kc_{167} cell line and put under normoxic or hypoxic conditions. The hypoxic cells showed a dramatic increase in GFP fluorescence compared to the normoxic cells (Fig. 2B). The hypoxic increase in GFP expression was eliminated by HIF-1α RNAi treatment. The original

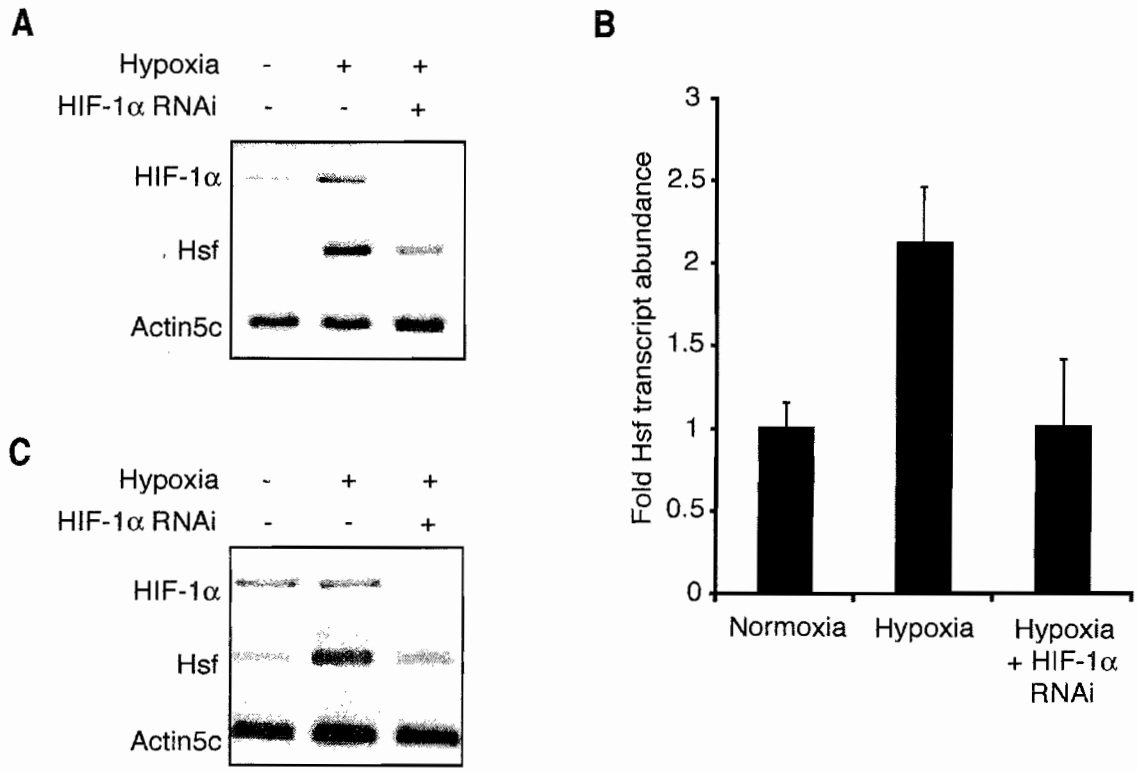

Figure 1. *Hsf* transcript levels are increased in a HIF-1α-dependent manner. A) RT-PCR analysis of the abundance of transcripts encoding HIF-1α, Hsf and Actin5c (control) during normoxia or hypoxia in Kc_{167} cells. *Hsf* is up-regulated after hypoxia and RNAi inactivation of HIF-1α eliminates this up-regulation. B) Real-time PCR experiments confirm that RNAi inactivation of HIF-1α reduces the up-regulation of *Hsf* after hypoxia. Standard error of the mean is shown. Transcript changes in each condition are significantly different ($p < 0.05$). C) RT-PCR analysis of the abundance of transcripts during normoxia or hypoxia. An alternate dsRNA sequence targeting HIF-1α for RNAi showed similar results as in (A) reducing the possibility that results from the original RNAi were due to non-specific effects.

reporter vector lacking the *Hsf* intron showed no hypoxic activation of GFP (data not shown), confirming that it was the cloned intronic region of *Hsf* that was leading to the HIF-1-dependent induction of the reporter during hypoxia.

The HRE-containing region was also tested for direct binding by HIF-1 by chromatin immunoprecipitation. We transfected Kc_{167} cells with a epitope-tagged HIF-1α expression vector (58). DNA bound to HIF-1 protein during hypoxia was immunoprecipitated and the *Hsf* intron genomic region as well as control genomic regions were PCR amplified to test for enrichment compared to DNA immunoprecipitated from a mock transfection. We found distinct enrichment of a 260-bp fragment encompassing the two HREs of the *Hsf* intron (Fig. 2C). As a positive control we showed an enrichment of a genomic region containing an HRE within the intron of the known HIF-1 target *Hph*. A negative control fragment located in an *Actin5c* intron showed no enrichment between the HIF-1α pull-down and the untransfected pull-down. These data indicate that *Hsf* is a direct target of HIF-1α through the binding of an intronic region containing two HREs that act as an enhancer of transcription during hypoxia.

Full induction of Hsps during hypoxia is dependent on HIF-1α regulation of Hsf

The functional impact of the up-regulation of *Hsf* by HIF-1α on Hsp induction during hypoxia was then assayed. Kc_{167} cells were exposed to normoxia and hypoxia after treatment with control and HIF-1α RNAi and reverse transcription-PCR assayed

transcript levels of various Hsps. All *Hsps* examined were dramatically up-regulated under hypoxia and this increase was partly HIF-1α-dependent (Fig. 3A). Hsp transcripts

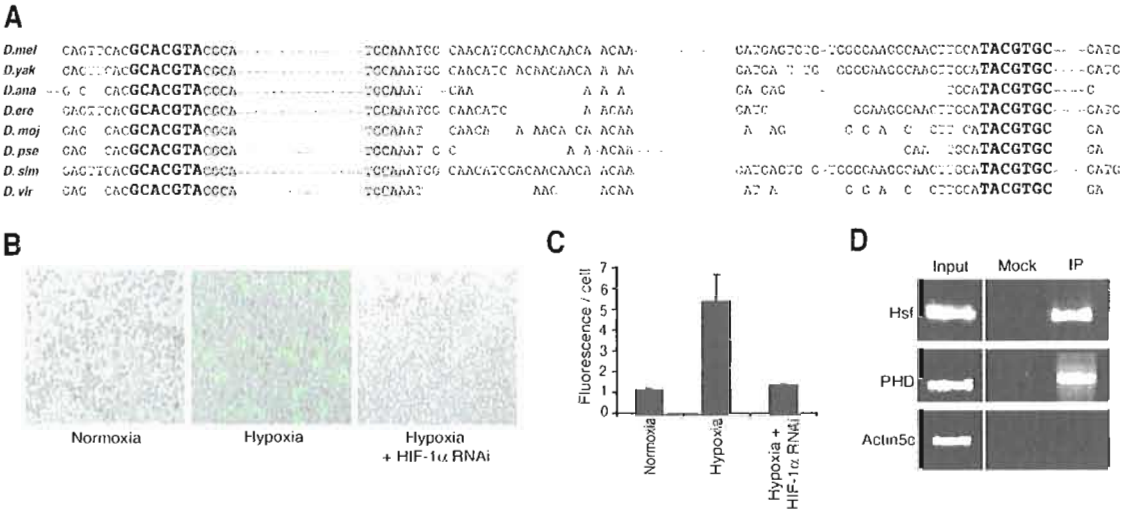

Figure 2. The *Hsf* gene region has conserved HREs and is a direct target of HIF-1. A) An alignment of the nucleotide sequence of the second intron the *Hsf* gene in eight *Drosophila* species shows two HREs are fully conserved. B) The genomic sequence containing the two HREs in the *Hsf* intron were cloned up-stream of the minimal promoter of the Green H Pelican reporter vector. This construct was transfected into Kc_{167} cells split into three conditions: normoxia, hypoxia or hypoxia with HIF-1α RNAi. The reporter was not activated by normoxia but hypoxia induced expression of the GFP reporter. The hypoxia activation of the reporter was eliminated by the addition of HIF-1α RNAi. C) Fluorescence was measured using an ISS PC1 spectrofluorometer and normalized by cell number. Quantification confirmed a significant increase in fluorescence during hypoxia and a significant decrease from the hypoxic induction when HIF-1α RNAi was added to hypoxic cells. D) Chromatin immunoprecipitation and PCR showing enrichment of the genomic region containing the two HREs within the *Hsf* gene in epitope-tagged HIF-1α transfected versus untransfected Kc_{167} cells. The *Hph* gene and *Actin5c* genes were used as positive and negative controls respectively.

were not completely eliminated in hypoxic cells treated with HIF-1α dsRNA, presumably because the hypoxic stress activated the basal (normoxic) levels of Hsf protein already present in the cells. No HREs were found near any of the *Hsp* genes, therefore it is unlikely that HIF-1 was directly up-regulating these genes during hypoxia.

We tested if the up-regulation of *Hsps* during hypoxia was dependent on Hsf. Cells were treated with control or Hsf RNAi and placed in normoxic and hypoxic conditions. When Hsf was removed through RNAi, Hsp transcripts were eliminated completely, compared to the strong induction seen in cells treated with control dsRNA (Fig. 3B). Real-time PCR was used to more accurately quantify the results from both of the RNAi experiments. HIF-1α RNAi reduced the up-regulation of Hsps during hypoxia, yet Hsf RNAi completely removed Hsp transcripts (Fig. 3C). From these results, we can discern that Hsf regulates *Hsps*, while HIF-1 regulates *Hsf*.

The lack of strong *Hsp* up-regulation in hypoxic HIF-1 knockdown cells suggests that the HIF-1-mediated increase in Hsf transcript levels is an important step in regulating the sensitivity and activity of the heat shock response pathway. The functional impact of an increase in Hsf transcript levels in hypoxia was tested by assaying the response to hypoxia of a fly heterozygous for the null Hsf^1 mutation (59), and therefore containing only a single wild-type copy of *Hsf*. After exposure to hypoxia, these flies had reduced levels of Hsf transcripts compared to wild-type Oregon R flies as measured by real-time PCR (Fig. 4). The heterozygous flies with a reduction in Hsf transcripts also showed a strong reduction in Hsp26, Hsp27 and Hsp68 transcript levels compared to the control flies, although two *Hsp70* genes had normal levels of induction.

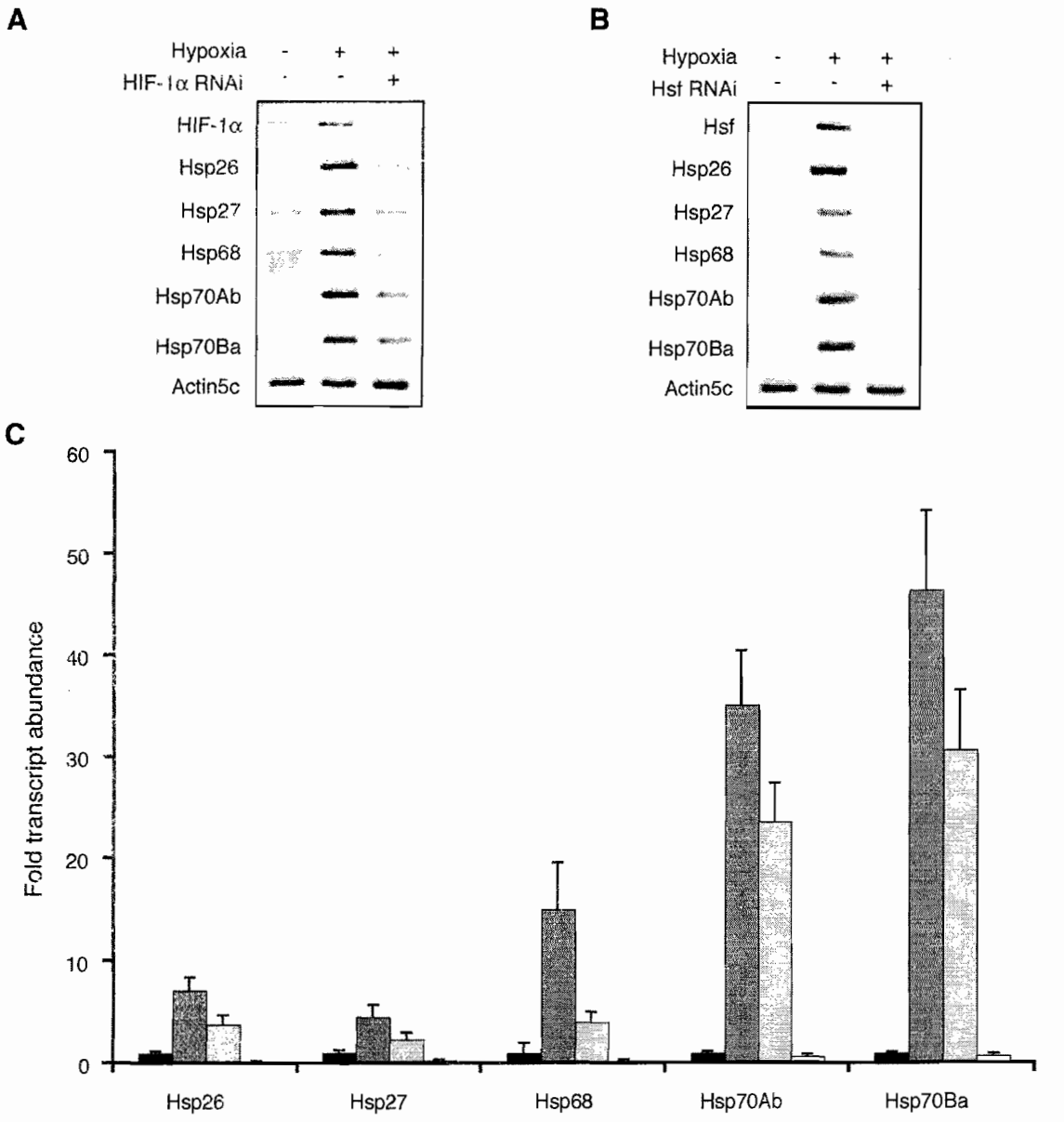

Figure 3. *Hsp* transcript levels are increased in an Hsf and HIF-1α-dependent manner during hypoxia. A) RT-PCRs of transcripts involved in the heat shock pathway are up-regulated after hypoxia. Inactivation of HIF-1α reduces the increase in Hsp transcripts. Actin5c is used as a control. B) RNAi of Hsf eliminates up-regulation of *Hsps* completely. C) Real-time PCR analysis of transcripts from normoxic cells (black bars), hypoxic cells (dark grey bars), hypoxic cells treated with HIF-1α RNAi (light grey bars) and hypoxic cells treated with Hsf RNAi (white bars). Hsp transcripts were normalized to normoxic levels. RNAi treatments reduced the transcripts Hsps compared to hypoxia alone ($p < 0.05$).

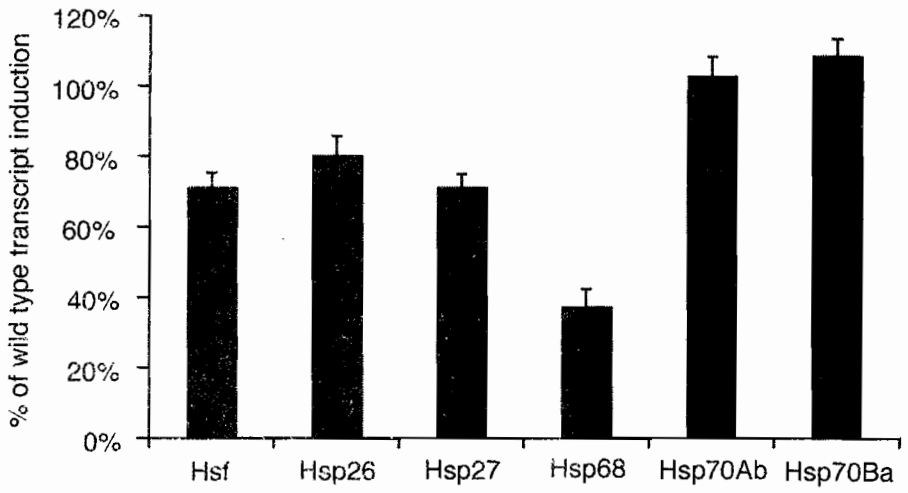

Figure 4. Up-regulation of *Hsps* is Hsf dosage-dependent. Real-time PCR of flies heterozygous for a null *Hsf* mutation show a significant reduction in Hsf, Hsp26, Hsp27 and Hsp68 transcript abundance compared to wild-type flies after hypoxia ($p < 0.05$). This demonstrates that Hsf transcript abundance is critical to the magnitude of Hsp production. Standard error of the mean is shown.

These findings suggest that Hsf abundance impacts the up-regulation of some *Hsps* in a dose-dependent manner during hypoxia. Lower Hsf transcript abundance than the levels normally achieved during hypoxia are insufficient for the full up-regulation of *Hsps*.

Full induction of Hsps and viability during reoxygenation is dependent on increased Hsf levels

During the return to normal oxygen conditions, Hsp levels remain high and are critical to tissue survival during this reoxygenation (60) (61). The effect of the HIF-1-dependent increase in Hsf level on Hsp expression persists during reoxygenation. Kc_{167}

tissue culture cells with HIF-1α knocked down by RNAi had little increase in Hsp expression after hypoxia treatment and a reoxygenation period (Fig. 5A). Thus, the up-regulation of *Hsf* during hypoxia is critical to the high levels of Hsp transcripts during reoxygenation, as well as hypoxia.

Furthermore, we examined the functional importance *in vivo* of increased Hsf transcript abundance by assaying larval survival under hypoxia and reoxygenation stress. First instar larvae were reared in a regime of alternating hypoxia and reoxygenation. The Hsf^{1} heterozygotes had greatly reduced survival compared to larvae reared in normoxia (Fig. 5B). Control wild-type larvae showed no significant difference in survival between normoxia and the hypoxia and reoxygenation environments. These findings demonstrate the dosage importance of Hsf transcript levels for coping with hypoxia and reoxygenation at the organismal level.

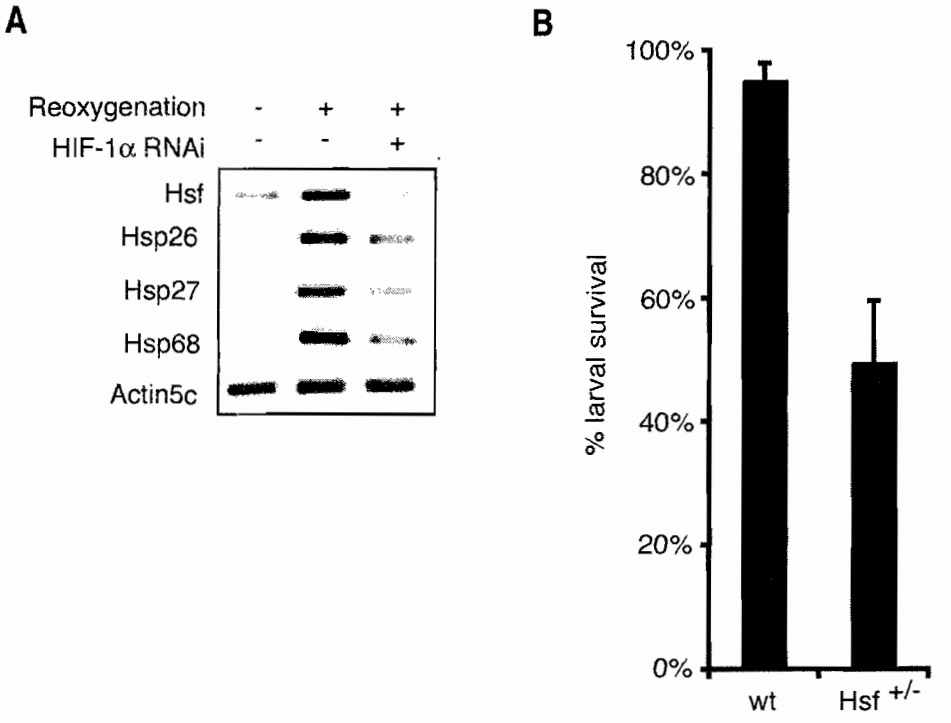

Figure 5. Up-regulation of *Hsps* after reoxygenation is HIF-1α-dependent and critical to survival. A) RT-PCR of transcripts involved in the heat shock pathway are up-regulated after hypoxia. HIF-1α RNAi reduces the increase in Hsp transcripts. Actin5c used as a control. B) Larvae reared in either normoxia or hypoxia with a reoxygenation period each day were allowed to develop into pupae. Development of wild-type larvae was minimally affected by the hypoxic and reoxygenation stress. However, half as many *Hsf* $^{+/-}$ larvae reached the pupal stage when faced with repetitive hypoxia and reoxygenation compared to normoxic larvae. The reduction in survival was significant ($p < 0.05$). Standard error of the mean is shown.

Taken together these experiments show the sequential order and importance of the hypoxia response. During hypoxia, HIF-1 directly up-regulates *Hsf*, which in turn up-regulates the whole family of *Hsps*. Without the HIF-1 regulated increase in Hsf, Hsps transcript levels never reach full induction during hypoxia or reoxygenation, and organismal viability is reduced.

Discussion

Up-regulation of *Hsps* during hypoxia is part of the canonical low-oxygen stress response seen in *Drosophila* (16), *C. elegans* (47), and mammalian tissues (62). This study provides evidence that the up-regulation of *Hsf* during hypoxia surprisingly requires the activity of HIF-1, the effector of the low oxygen response. The transcriptional control of *Hsf* by HIF-1 has a functional impact on the activity of the heat shock response during hypoxia and the return to normal oxygen levels. Cells lacking HIF-1 or with reduced dosage of Hsf only increase Hsp transcript production slightly during low oxygen exposure and reoxygenation. The decreased production of Hsps reduces viability in flies experiencing hypoxia and reoxygenation, demonstrating that the full induction of the heat shock response is essential to counter the diverse physiological stresses associated with low oxygen.

Thus, we propose a model where HIF-1 directly up-regulates *Hsf* during hypoxia, and the increased Hsf abundance in turn allows Hsf to further up-regulate *Hsps* during low oxygen exposure and also after the return to normal oxygen levels. The regulation of *Hsf* by HIF-1 provides a clear example of how cross-regulation between physiological

stress response pathways can allow one pathway to sensitize the second and elicit a response under conditions where normally it would not be activated.

Complex regulation of physiological response pathways

Cross-regulation between physiological pathways appears to be a feature of the low oxygen response. It has been shown that the insulin pathway can dramatically affect the HIF-1 pathway (63). Through the actions of the phosphatidylinositol 3-kinase/Akt pathway, HIF-1α translation is increased in a manner that outpaces the naturally normoxic degradation of HIF-1α (64). This leads to HIF-1 activation even when oxygen is present and up-regulating its downstream targets. Recently, it has been shown that transforming growth factor-β1 activates the HIF-1 pathway by reducing the levels of prolyl hydroxylases that tag HIF-1α for degradation. Interestingly, it is also known that Hsp90 plays are role in stabilizing HIF-1α (65) (66). This mechanism is independent of the canonical oxygen-dependent regulation of HIF-1α and was the first evidence of any link between the heat shock and hypoxia stress pathways.

The cross-regulation between HIF-1 and Hsf found here is a new type of control, where the transcriptional effector of the low oxygen response directly regulates the transcript level of the effector of the heat shock response in order to sensitize the pathway. Interestingly, it has been already shown that HIF-1 and Hsf pathways have regulatory interactions, but in response to heat. Studies using *C. elegans* and rats showed that HIF-1 activity was essential for heat acclimation (67) (68). Our findings may explain the mechanism behind this phenomenon, in that the increase in metabolic activity

during high temperature may cause oxygen scarcity, thus stabilizing HIF-1 and increasing Hsf transcript levels.

Transcriptional control of the heat shock response

The activity of the heat shock pathway has been shown to be controlled by the trimerization and post-translational modification of Hsf protein subunits (51). Our results indicate that transcriptional control of *Hsf* is a means of further regulation of heat shock pathway activity. This transcriptional regulatory step is controlled by HIF-1, supporting a model in which the HIF-1 pathway causes increased *Hsf* transcription during hypoxia as a means to increase the cellular abundance of Hsf and increase the sensitivity of the heat shock pathway. In addition, the control of heat shock response sensitivity by HIF-1, the regulator of the low oxygen response, suggests that stress response pathways can assimilate complex new functions by regulating the transcriptional activators of other stress pathways.

Disease implications

It has been shown that the increase in Hsp levels are critical for cell survival during hypoxia and the subsequent reoxygenation (61) (69). Our results indicate that it is through the HIF-1 pathway that the cell achieves this Hsp increase and is a means to protect against the stress of hypoxia. HIF-1 accumulation and activity have been linked to tumor progression and various Hsps have also been shown to be crucial to cancer survival (70), thus, the hypoxic and heat shock response pathways play important roles in the pathophysiology of cancer. Our finding that the activity of HIF-1 controls the output

of the heat shock pathway offers possible therapeutic approaches for mitigating hypoxic tissue damage and tumor growth by targeting this novel regulatory link.

Methods

Cell culture and hypoxia treatments

Drosophila melanogaster Kc_{167} tissue culture cells were obtained from the *Drosophila* Genomics Resource Center. Cells were maintained in Schneider's *Drosophila* Medium (Gibco), supplemented with 5% heat-inactivated Fetal Bovine Serum (Gibco). For hypoxia experiments, cells were incubated for 6 hours in chambers flushed with 0.5% O_2 gas. The reoxygenation step consisted of a 15 minute return to normal oxygen levels.

RNA interference

RNAi was performed as previously reported (71). The following primer pairs were used to generate template DNA: control Green Fluorescent Protein (GFP) (5′-GCCACAAGTTCAGCGTGTCC and 5′-GCTTCTCGTTGGGGTCTTTC), HIF-1α (sima) (5′-CTGCGGGACTATCATAACAACC and 5′-AGGCTCAAAATCAATCTTTTGG), alternate HIF-1α (5′-GCATCACATCAAAGAGTCCCGAG and 5′-TCCGCAACCGTAACACCACTAC) and Hsf (5′-TGCCAAACAGTCCGCCTTATTAC and 5′-TGCTTTCCAAGTGCCCGTG). The T7 promoter sequence (5′-TAATACGACTCACTATAGGGAGA) was added 5′ to all above primers when ordered (IDT).

Reverse Transcription-PCR

Total RNA was isolated using standard Trizol protocols. Instructions from Superscript III One-Step RT-PCR System with Platinum Taq (Invitrogen) were followed using 1 μg of total RNA and 21 cycles of amplification were used for each test. The following primer pairs were used: HIF-1α (5′-CGAACTCGGTACTAAAGAACCTGC and 5′-GGGTCCTACTTTCACGCAAGG), Hsf (5′-ATCTGCTGCGTGGCGATG and 5′-CGTCCGTGTCCAAAATGTCG), Hsp26 (5′-ATGGCGTGCTCACCGTCAGTATTC and 5′-GGATGATGTTGGATGATGATGGCTC), Hsp27 (5′-AGGAGGAAGAAGACGACGAGATTCG and 5′-CATTGGGTGTGTTGTGGTGTGTCC), Hsp68 (5′-TTCACCACCTATGCCGACAACCAG and 5′-TCACATTCAGGATACCGTTTGCGTC), Hsp70Ab (5′-TCCATTCAGGTGTATGAGGGCG and 5′-CGTTCAGGATTCCATTGGCGTC), Hsp70Ba (5′-ACGATGCCAAGATGGACAAGGG and 5′-CGTCTGGGTTGATGGATAGGTTGAG) and Actin5c (5′-GGATGGTCTTGATTCTGCTGG and 5′-AGGTGGTTCCGCTCTTTTC).

Real-time PCR

Total RNA was isolated using standard Trizol protocols. cDNA was synthesized following the SuperScript III Reverse Transcriptase protocol (Invitrogen). Real-time PCR was performed using the Sybr Green PCR Master Mix (Applied Biosystems) and an

ABI PRISM 7900HT detection system (Applied Biosystems). The supplied analysis software was used for data interpretation. The following primer pairs were used: Hsf (5′-ACACCGCAGCCTCACATTATGACC and 5′-ATTTCCCTGGAGCAGCAAGTCCTC), Hsp27 (5′-AGGAGGAAGAAGACGACGAGATTCG and 5′-CATTGGGTGTGTTGTGGTGTGTCC), Hsp68 (5′-TTCACCACCTATGCCGACAACCAG and 5′-TCACATTCAGGATACCGTTTGCGTC), Hsp70Ab (5′-TCCATTCAGGTGTATGAGGGCG and 5′-CGTTCAGGATTCCATTGGCGTC), Hsp70Ba (5′-ACGATGCCAAGATGGACAAGGG and 5′-CGTCTGGGTTGATGGATAGGTTGAG) and Actin5c (5′-TGCTGGAGGAGGAGGAGGAGAAGTC and 5′-GCAGGTGGTTCGCTCTTTTCATC).

Hypoxia reporter construction

A small region of the *Hsf* intron containing the possible hypoxia regulatory elements was cloned into the Green H Pelican reporter vector. Kc_{167} cells were transfected using the Effectene kit (Qiagen) with this reporter and put in normoxia, hypoxia or hypoxia with HIF-1α RNAi. Images were taken using a Nikon Eclipse TE2000-U microscope and MetaVue image capture software.

Chromatin immunoprecipitation

Kc_{167} cells were transfected using the Effectene kit (Qiagen) with a pAc5.1/Sima plasmid, which contains the full-length HIF-1α (sima) cDNA sequence with a c-terminal V5 epitope tag under the control of the Actin5c promoter. An equal quantity of mock transfected cells was used as a control and all purification steps were carried out in parallel with the control and experimental cells. 24 hours after transfection, control and experimental cells were incubated in hypoxia at room temperature for 24 hours. DNA isolation and purification procedures followed standard V5 protocol.

PCR was used to detect *Hsf*, *Hph*, and *Actin5c* genomic regions in each of the samples of isolated DNA. 35 cycles were used to amplify 2 μl of template from each sample using the following primers: Hsf (5′-CTCCCACCACATACCGCTAATC and 5′-AAAAGCCAACTGAATGACCAAGG), Hph (5′-CCTTCTCACACTCCCTTCGCTG and 5′-CACTCTCTGCCAAGCCAAACC), Actin5c (5′-TGTGTGTGAGAGAGCGAAAGCC and 5′-CTGGAATAAACCGACTGAAAGTGG).

Larval survival

First instar larvae of wild-type or flies with only one copy of the *Hsf* gene were counted and placed 10 per vial of food. These vials were split and placed into groups for normoxic or hypoxia and reoxygenation stresses. This experimental group was maintained at 0.5% oxygen for 23 hours, then placed in ambient oxygen for one hour, before returning to hypoxia. This cycle was repeated daily and after two weeks the vials were scored for survival.

Bridge to Chapter IV

By identifying *HSF* as a target of HIF-1, we described a mechanism by which hypoxia activates a transcriptional response more commonly associated with heat stress. In Chapter IV, more cross talk between stress pathways is reported. Here, we showed that hypercapnia causes the repression of NF-κB-dependent antimicrobial gene expression.

CHAPTER IV

ELEVATED CO_2 SUPPRESSES SPECIFIC *DROSOPHILA* INNATE IMMUNE RESPONSES DOWNSTREAM OF NF-kB PROTEOLYTIC ACTIVATION

Reproduced from I.T. Helenius*, T. Krupinski*, D.W. Turnbull, Y. Gruenbaum, N. Silverman, E.A. Johnson, P.H.S. Sporn, J.I. Sznajder, G.J. Beitel. Submitted to *Journal of Experimental Medicine*, 2008
*Authors contributed equally to this work

I performed the experiments and analyzed the data for the gene expression microarray results described in this paper. I also helped with interpretation of the data and the design of subsequent experiments based on it.

Although an average human produces 450 liters of CO_2 per day (72) and elevated levels of CO_2 (hypercapnia) in the pulmonary and/or circulatory system are associated with worse outcomes in chronic obstructive pulmonary disease (COPD) (73) (74), the cellular pathways that sense and respond to CO_2 are poorly understood (reviewed in (75) (76)) and a comprehensive description of a CO_2 response pathway is lacking in any system. We sought to develop a genetically and molecularly tractable system for defining non-neuronal CO_2 response pathways and chose *Drosophila* because of extensive conservation of the hypoxia (31), nitric oxide (NO) (77) and nearly all other major signal

transduction pathways between *Drosophila* and mammals. Further, *Drosophila* possess a well-characterized, multi-component innate immune system controlled by conserved signaling pathways that include NF-kB-family transcription factors (78). Genetic and high throughput RNAi studies using whole flies and S2 cell culture have contributed to understanding the human innate immune system (reviewed in (79)), including identification of Toll, the founding member of the Toll-like-receptor (TLR) family, and most recently of the Akirin proteins that are required for NF-kB-dependent gene expression (80).

In this report we show that *Drosophila* have specific physiological responses to hypercapnia which include a suppression of particular NF-kB-regulated antimicrobial peptides that is remarkably parallel to the suppression of specific NF-kB-regulated innate immune/inflammatory cytokines in human macrophages (see accompanying report by Wang *et al.* [ref]). These results establish *Drosophila* as a general model for defining non-neuronal CO_2 signaling pathways and as a specific model for investigating suppression of NF-kB effectors by hypercapnia.

Results and Discussion

Hypercapnia causes specific effects on Drosophila physiology independent of known neuronal CO_2 sensing pathways.

To determine whether hypercapnia affects *Drosophila* physiology, we exposed flies to 13% and 19.5% CO_2 (~pCO_2 94 and 140 mmHg), while maintaining O_2 at 21% (see Materials and methods). These CO_2 levels are well below the ~30% concentration at which CO_2 becomes anesthetic. Hypercapnia causes dose-dependent defects in

embryonic development. 13% CO_2 results in 20% of embryos having moderate defects such as malformations of the airway system (compare Fig. 1A and B) and also significantly slows hatching of eggs laid by normocapnic mothers (Fig. 1D,E). 19.5% CO_2 severely disrupts embryonic development with ~30% of exposed embryos showing large-scale patterning and morphogenesis defects (Fig. 1C), and more than 70% of eggs failing to hatch (Fig. 1E). In contrast, adult *Drosophila* survive exposure to 13% and 19.5% CO_2 for many weeks (data not shown), consistent with the essentially normal postnatal development of mice exposed to 12% CO_2 (81). The effects of hypercapnia on vertebrate embryonic development have not been reported, but these results suggest that embryonic and adult metazoans may have different sensitivities to hypercapnia. However, exposure of adult flies to hypercapnia is not without adverse consequences, as hypercapnia causes a dose-dependent reduction in the number of eggs females lay (Fig. 1F). Importantly, flies homozygous for a null mutation in the neuronal CO_2 receptor Gr63a (82) (83) are as sensitive to hypercapnia as wild-type flies in the egg hatching and laying assays (Fig. 1D-F). Thus, many physiological effects of hypercapnia are mediated by an as yet uncharacterized CO_2 response pathway(s).

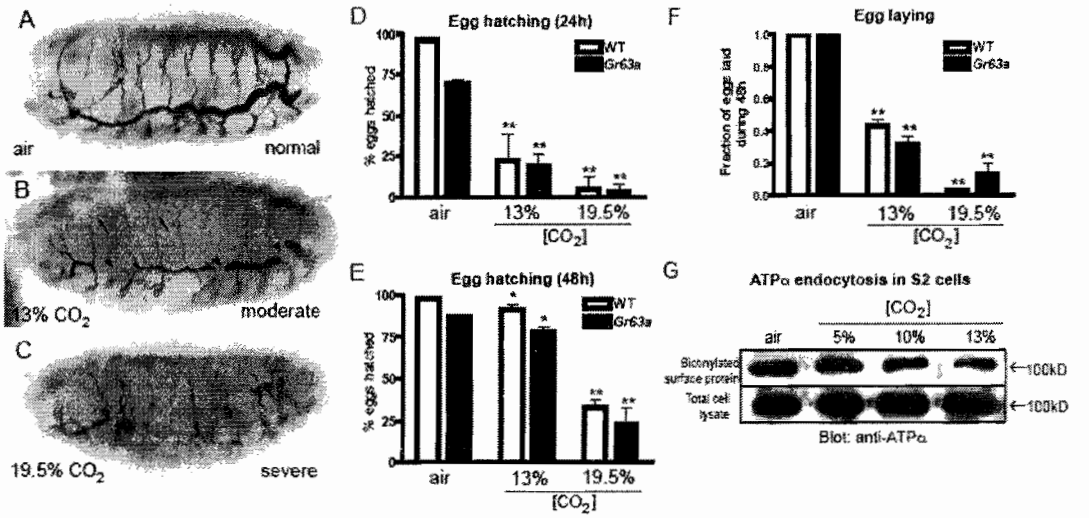

Figure 1. Hypercapnia affects *Drosophila* development and physiology independently of neuronal CO_2 sensing. (A-C) *Drosophila* embryonic development is disrupted by hypercapnia. The embryonic tracheal (airway) system, visualized by a lumenal stain, is an excellent readout of general morphogenesis because tracheal branch guidance requires interaction with multiple tissues. Culturing wild-type embryos in 13% CO_2 causes moderate defects in 20% of embryos (B, n=111), while 19.5% CO_2 causes severe defects in 28% of embryos (C, n=71) and increases the prevalence of moderate defects to 41%. Moderate defects (B) include breaks in the main airways (arrowheads) and missing or ectopic interconnections of dorsal branches (arrows), while severely abnormal tracheal development reveals gross embryonic patterning and/or morphogenesis defects (C). (D,E) Hypercapnia (24h, D) decreases hatching of eggs laid in normocapnia by wild-type (WT) or mutant flies homozygous for a null allele in the neuronal CO_2 receptor, Gr63a. In 13% CO_2 over 90% of WT embryos hatch after 48h (E), but in 19.5% CO_2 only ~30% hatch. (F) Hypercapnia reduces the number of eggs laid in 48h by WT and *Gr63a* females mated in normocapnia. (G) As in mammalian cells hypercapnia (1h) causes endocytosis of the Na,K-ATPase in S2 cells. * = $p < 0.05$, ** = $p < 0.005$ between CO_2 condition and air; error bars are standard deviation.

We next asked whether *Drosophila* share with mammals any specific response to hypercapnia. We previously reported that in human alveolar epithelial cells, hypercapnia causes endocytosis of the Na,K-ATPase (84). Analysis of surface abundance of Na,K-ATPase in *Drosophila* S2 cells reveals that hypercapnia also causes dose-dependent endocytosis of the sodium pump in S2 cells (Fig. 1G). As Gr63a is expressed only in specific CO_2-sensing olfactory neurons (82), the responsiveness of the hematopoietic S2 cell line to hypercapnia further supports the existence of cell autonomous CO_2 responses that do not depend on the neuronal Gr63a sensing pathway. That both *Drosophila* and

human cells endocytose their Na,K-ATPase in response to hypercapnia suggests that some CO_2 responses are conserved between mammals and flies.

Hypercapnia causes specific effects on gene expression

To investigate the molecular basis of the physiological effects of hypercapnia and to identify CO_2-responsive promoters to use as markers for dissecting CO_2 signaling pathways, we next performed microarray analysis on adult flies. Similar to the limited changes in gene expression seen in neonatal mice raised in CO_2 (81), exposure of adult flies to 24h of 13% CO_2 causes fewer than 500 genes to be up- or down-regulated more than 1.5-fold, and fewer than 10 by more than 10-fold (data not shown). Therefore, in *Drosophila* CO_2 causes specific rather than global changes in gene expression. Consistent with the dramatic decrease in fecundity of female flies during hypercapnia, the chorion and vitelline membrane genes required for egg production are among the genes most highly down-regulated by elevated CO_2 (Table S1). Notably, CO_2 does not induce genes characteristic of hypoxic, heat shock or oxidative stress responses (Table S1), indicating that the responses to elevated CO_2 are mediated by distinct pathways. Most intriguingly, a subset of the antimicrobial peptide (AMP) genes that are effectors of the *Drosophila* innate immune system are down-regulated by elevated CO_2 levels (Fig. 2A). Given the prevalence of pulmonary infections in hypercapnic COPD patients (85), we focused on defining the effects of hypercapnia on the highly conserved NF-kB-regulated innate immune system of *Drosophila* and determining whether hypercapnia could render a host more susceptible to infection by a pathogen.

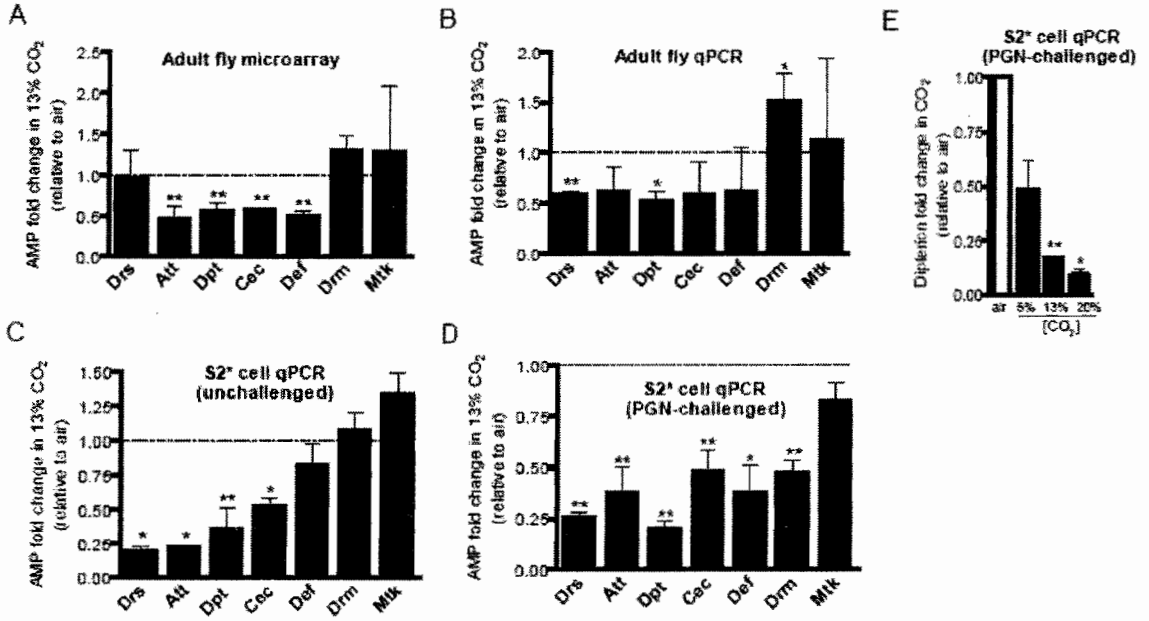

Figure 2. Hypercapnia down-regulates specific antimicrobial peptides in *Drosophila*
(A-B) Hypercapnia (24h) suppresses specific antimicrobial peptides (AMPs) *in vivo* in unchallenged adults as shown by microarray analysis (A) and confirmed by quantitative PCR (B). (C-D) Hypercapnia suppresses specific AMPs *in vitro* (10h CO_2 for C,D; PGN challenge at 5h in D). (E) Suppression of the AMP Diptericin by hypercapnia in S2* cells is dose-dependent. Protein levels of AMPs were not assessed because antibodies against *Drosophila* AMPs are not available. * = $p < 0.05$, ** = $p < 0.005$ between CO_2 condition and air; error bars are standard deviation. PGN = *E. coli* peptidoglycan; Drs = Drosocin; Att = Attacin; Dpt = Diptericin; Cec = Cecropin; Def = Defensin; Drm = Drosomycin; Mtk = Metchnikowin.

Hypercapnia suppresses select antimicrobial peptide genes in vivo *and* in vitro

We confirmed and extended our microarray results using quantitative real-time reverse transcriptase PCR (qPCR) and found that hypercapnia indeed suppresses expression of many AMPs in adult flies (Fig. 2B). To identify a simplified *in vitro* system for investigating hypercapnic immune suppression, we tested the effects of hypercapnia on the expression and induction of AMPs in *Drosophila* S2* cells, a macrophage-like cell line whose viability is unaffected by 13% CO_2 (Table S2). Consistent with the adult fly data, exposing S2* cells to 13% CO_2 in the absence or presence of immune challenge significantly suppresses the expression of a subset of AMPs (Figs. 2C,D,S1). Notably,

Diptericin (Dpt) and Attacin, canonical effectors of the TNF-like IMD pathway (78), are consistently suppressed 3- to 5-fold. In contrast, Metchnikowin is not suppressed by hypercapnia. The effects of hypercapnia on AMPs are dose-dependent, and even a modest 5% CO_2 causes a 50% suppression of Dpt induction in response to PGN (Fig. 2E). As the bulk of AMPs in adult flies are produced by the fat body, the fly's functional equivalent of a liver, the similar effects of hypercapnia on AMP expression in whole flies and in S2* cells suggests that the effects of hypercapnia on the innate immune system affect multiple cell types. Thus, these results establish S2* cells as a powerful *in vitro* tool for defining the molecular details of CO_2 response pathways.

Hypercapnia increases susceptibility of Drosophila *to specific bacterial infections*

Antimicrobial peptides are a crucial element in the fly's defense against pathogens as mutations that decrease AMP production decrease resistance to infection (86). We therefore asked if hypercapnic suppression of AMPs reduces the ability of flies to survive infection with bacteria, including the natural *Drosophila* pathogen *E. faecalis* (87), and a human pathogen commonly isolated from COPD patients, *S. aureus* (88). Elevated CO_2 does not decrease survival from inoculation with sterile PBS (Fig. 3A) or with *E. coli*, which is not a *Drosophila* pathogen (Fig. 3B). However, at 13% CO_2, flies show significantly increased mortality when infected with *E. faecalis* (Fig. 3C). Strikingly, CO_2 levels as low as 7% increase mortality to *S. aureus* (Fig. 3D).

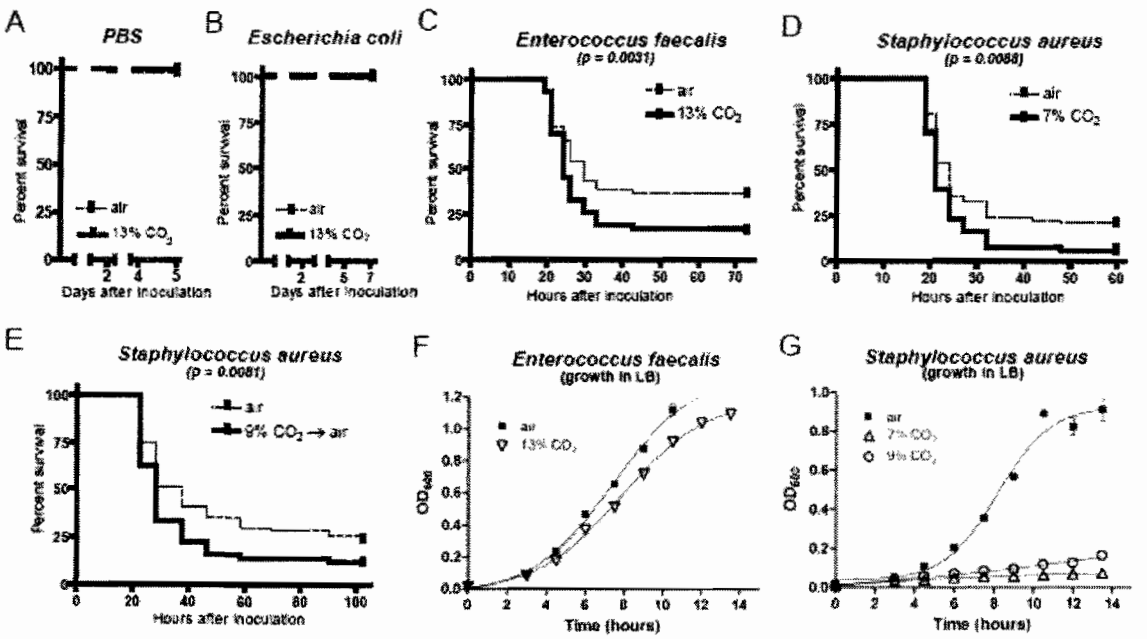

Figure 3. Hypercapnia increases mortality of bacterial infection in *Drosophila*. (A-D) Hypercapnia does not increase mortality of flies inoculated with PBS (A) or with *E. coli* (B), which is not a *Drosophila* pathogen, but does significantly increase mortality after inoculation with the *Drosophila* natural pathogen *E. faecalis* (C), or the human opportunistic pathogen *S. aureus* (D) at CO_2 levels as low as 7%. Unless otherwise noted, flies were exposed to indicated CO_2 level for 24h before inoculation and returned to hypercapnia until end of assay. We show representative results for the lowest CO_2 levels at which significant effects on mortality were consistently observed. All experiments were done in triplicate and the trial with the middle p-value is shown. (E) Pre-treatment of flies with 9% CO_2 prior to *S. aureus* infection in air is sufficient to increase mortality even when flies are cultured in air during and after inoculation. (F,G) Effects of hypercapnia on bacterial growth. Note that *S. aureus* growth is dramatically reduced in 7% CO_2 even though hypercapnia increases mortality of flies infected with *S. aureus*. Error bars smaller than the data-point symbols are not shown. (A-E) Kaplan-Meier survival curves, p-value determined by log-rank analysis.

Although the above results demonstrate that hypercapnia can decrease survival during infection, they do not distinguish whether decreased survival results from suppression of host defense, from enhanced bacterial pathogenicity, or both. We definitively demonstrate that increased mortality results at least in part from direct effects of CO_2 on the fly immune system by exposing flies to 9% CO_2 for 24h and returning them to normocapnia after inoculation with *S. aureus*. This hypercapnic pre-treatment of the host significantly increases mortality after pathogen infection although the pathogen was never exposed to hypercapnia (Fig. 3E).

We also investigated whether hypercapnia alters bacterial growth rates. Growth of *E. faecalis* in media is not significantly affected by elevated CO_2 (Fig. 3F). However, despite the markedly increased mortality of *S. aureus*-infected flies, growth of *S. aureus* is actually reduced several-fold by even 7% CO_2 (Fig. 3G). As decreased bacterial growth would have been expected to improve fly survival, the observed increase in mortality further supports the conclusion that hypercapnia suppresses *Drosophila* innate immune responses.

Importantly, the decreased growth rates of some bacteria in elevated CO_2 may provide an explanation for the existence of hypercapnic immune suppression. Because hyperactivation of immune responses in *Drosophila* or humans can cause pathology beyond that of an infection alone, immune responses may be deliberately attenuated during hypercapnia to prevent overreaction when pathogen growth is reduced. The observed increase in mortality during hypercapnia could result from an imperfect match between the degree of immune suppression and changes in bacterial growth. Another, and not exclusive, possibility is that CO_2 serves as a readout of metabolic activity with

elevated CO_2 indicating excessive metabolic load. Thus, hypercapnia may suppress select metabolically demanding functions including immune responses (89) and egg-laying to allocate energy to more immediate needs such as powering the flight muscles, which are among the most metabolically active tissues known.

Hypercapnia suppresses, not delays, innate immune responses

To further investigate the nature of hypercapnic immune suppression, we determined how hypercapnia affects the kinetics of innate immune responses. Hypercapnia does not alter the timing of AMP induction in PGN-challenged S2* cells, but the magnitude of the responses at any time is reduced (Fig. 4A). Thus, hypercapnia suppresses rather than delays innate immune responses. In S2* cells, this suppression exhibits rapid onset and recovery, as shifting cells from air to 13% CO_2 simultaneous with PGN challenge causes a two-fold reduction in Dpt induction, and increasing the pretreatment time beyond 5h does not further increase the suppression (Fig. 4B). Conversely, CO_2-treated cells challenged upon shift to normocapnia have normal induction of Dpt (Fig. 4C). The effects of hypercapnia on AMP induction in S2* cells closely parallel the effects on cytokines in human macrophages as detailed in the accompanying report by Wang et al [ref], supporting the existence of a conserved molecular mechanism of hypercapnic immune suppression.

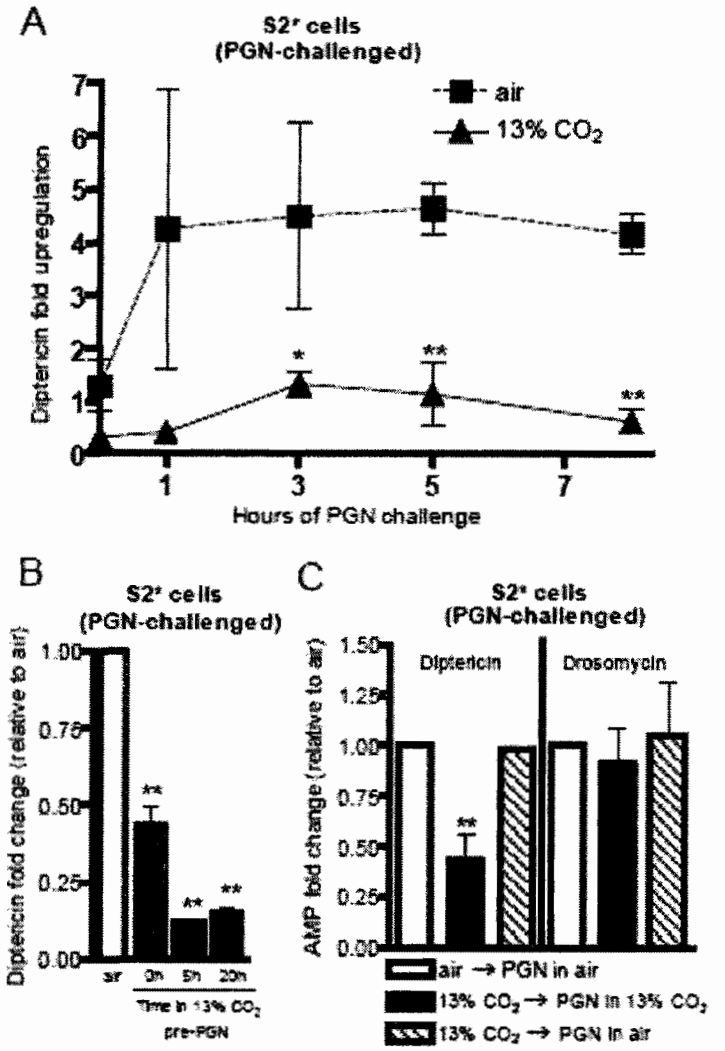

Figure 4. Hypercapnia suppresses antimicrobial peptide induction with rapid onset and recovery. (A) Hypercapnia suppresses, not delays, antimicrobial peptide (AMP) induction *in vitro* as assayed by qPCR of Diptericin (Dpt) in PGN-challenged S2* cells. (B) qPCR of Dpt in PGN-challenged S2* cells shows that the onset of immune suppressive effects of hypercapnia is rapid as shifting cells to hypercapnia at the time of PGN challenge results in ~50% suppression of Dpt with maximal suppression reached by 5h. (C, Left) Recovery from immune suppression is also rapid as challenging S2* cells with PGN in air immediately after removal from CO_2 results in full induction of Dpt. (C, right) As in unchallenged flies and S2* cells, Drosomycin is not strongly regulated by hypercapnia. * = $p < 0.05$, ** = $p < 0.005$; error bars are standard deviation.

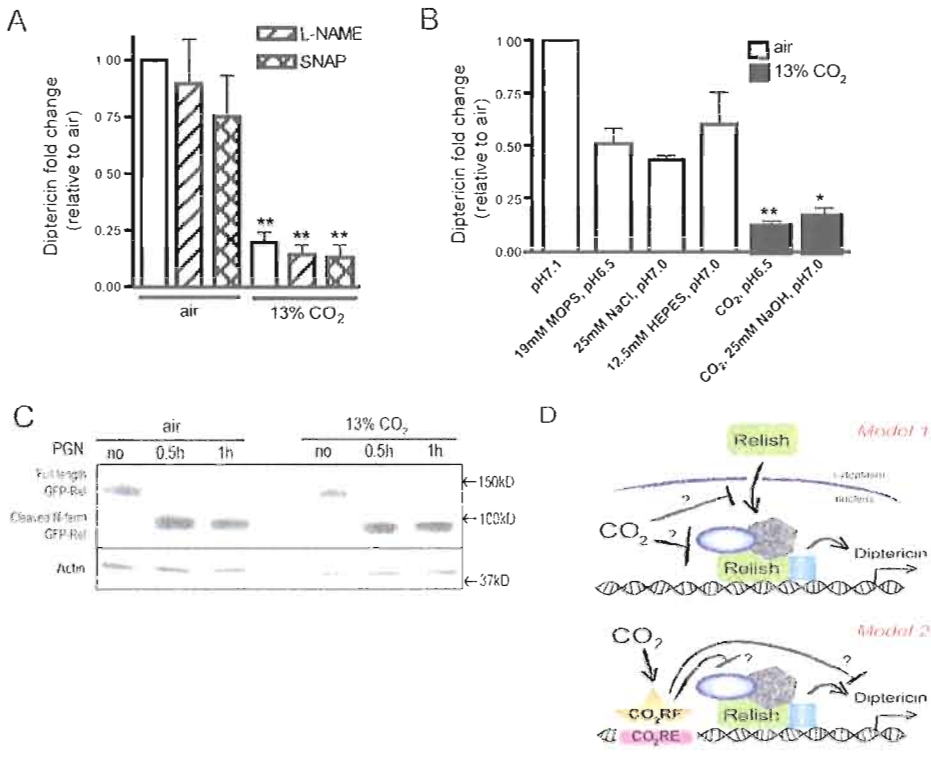

Figure 5. Hypercapnia suppresses innate immune responses via a novel pathway.
(A) Suppression of Diptericin (Dpt) in PGN-challenged S2* cells is not attenuated or enhanced by the NO synthase inhibitor L-NAME (1mM) or the NO donor SNAP (1mM). (B) Hypercapnia suppresses Dpt induction five-fold when the culture medium is adjusted to pH7.0 with NaOH, but Dpt induction is only suppressed ~two-fold by MOPS at pH6.5 and by NaCl and HEPES at pH7.0. (C) Hypercapnia does not alter Relish (Rel) cleavage in response to PGN challenge. GFP immunoblot of whole-cell lysates of S2 cells expressing GFP-Rel. (D) Models for hypercapnic suppression of innate immune effectors. Model 1: a hypercapnia response pathway modulates the nuclear import or activity of either Rel or a component of the Rel transcriptional complex, thus reducing Dpt expression. Model 2: analogous to the regulation of hypoxia responsive genes by the HIF transcription factor {Semenza, 2007, Sci STKE, 2007, cm8}, a CO_2 response pathway activates a hypothetical CO_2 responsive factor (CO_2RF) that binds specific CO_2 response elements (CO_2RE), inhibiting the Rel complex or directly suppressing Dpt expression. The conceptual difference between the two models is that, in model 1, genetic removal of the component of the Rel complex targeted by the CO_2 response pathway would significantly alter Dpt transcription even in the absence of CO_2. In contrast, removal of the CO_2 responsive factor in model 2 would render the promoter unresponsive to CO_2 regulation without affecting basal or induced transcription of Dpt in ambient air. * = $p < 0.05$, ** = $p < 0.005$ between CO_2 condition and equivalently treated air condition (A) or untreated air condition (B); error bars are standard deviation.

Hypercapnic immunosuppression is not mediated by nitric oxide or acidosis

As discussed above, the effects of hypercapnia on *Drosophila* physiology and the immune responses of S2 cells are not mediated via neuronal CO_2 sensing, and hypercapnia acts via pathways distinct from hypoxia, heat shock and oxidative stress. Because no non-neuronal CO_2 sensing pathways have been defined, we tested possible roles of candidate signaling pathways in hypercapnic immune suppression. NO has important roles in innate immune function in *Drosophila* and mammals (77) (90), and hypercapnia has been proposed to modulate NO-dependent pathways and inflammatory oxidants (91) (92). However, NO does not mediate hypercapnic immune suppression because hypercapnic suppression of Dpt in S2* cells is unaffected by either an NO synthase inhibitor or an NO donor (Fig. 5A).

Another candidate mediator of hypercapnic effects is acidosis, because CO_2 reacts with water to form carbonic acid ($H^+CO_3^-$). However, hypercapnic immune suppression is unlikely to result from sustained intracellular acidosis as we have previously shown that in primary mammalian alveolar epithelial cells hypercapnia causes only a minutes-long drop in intracellular pH (93). Here we show that extracellular acidosis does not account for hypercapnic immune suppression in S2* cells because acidifying S2* culture media with 19mM MOPS in normocapnia causes only a ~two-fold suppression of Dpt expression that is less than half that caused by 13% CO_2 (Fig. 5B). Notably, 25mM NaCl or HEPES at neutral pH causes suppression equal to that of acidosis, making it difficult to discern acidotic from ionic or non-specific effects. We definitively demonstrate effects of CO_2 independent of extracellular acidosis by maintaining the S2* cell media at neutral

pH during exposure to 13% CO_2 and finding that hypercapnia suppresses Dpt induction to the same extent seen in hypercapnic acidosis (Fig. 5B, black bars). Similarly, Wang *et al.* [ref] show that hypercapnia suppresses innate immune responses of human alveolar macrophages even when extracellular acidosis is neutralized. Thus, in both flies and mammals, hypercapnia has a unique and consistent pattern of immune suppression distinct from the effects of extracellular acidosis.

Hypercapnia acts downstream of, or in parallel to, NF-kB activation

How does hypercapnia modulate innate immune responses? In S2 cells, induction of AMPs by *E. coli* PGN is entirely dependent on the TNF-like IMD pathway Rel/NF-kB factor Relish (Rel) (94) (95). Rel contains an N-terminal Rel homology domain (RHD), which is endoproteolytically cleaved from a C-terminal inhibitory IkB-like region in response to PGN stimulation (96). In S2 cells exposed to 13% hypercapnia, there is no reduction in the PGN-induced proteolytic cleavage of Rel (Fig. 5C). Therefore, hypercapnia inhibits expression of Rel targets downstream of proteolytic activation either by acting on one of the components of the Rel transcription complex (Fig. 5D, model 1), or on unidentified transcriptional complexes acting in parallel to Rel (Fig. 5D, model 2). Although further work is required to elucidate the exact mechanism, together with the work of Wang *et al.* in mammalian macrophages showing that hypercapnia suppresses NF-kB targets without blocking proteolytic activation of RelA, our combined results suggest that this mechanism is conserved.

Concluding Remarks

Hypercapnic suppression of innate immune and inflammatory responses has important implications for human health. Previous reports have suggested that hypercapnia can have beneficial effects when "permissive hypercapnia" regimens are used during mechanical ventilation (97), and hypercapnic suppression of NF-kB-mediated inflammatory responses may account for the favorable outcomes observed when CO_2 is used as an inflatant in laparoscopic surgery (98). However, suppression of innate immune responses by hypercapnia in *Drosophila* as well as in a recent bacterial pneumonia model in rats (99) is highly suggestive of elevated CO_2 causally contributing to worse outcomes of hypercapnic COPD patients by promoting bacterial infections and exacerbations. The current lack of understanding of the molecular pathways that mediate CO_2 responses severely limits our ability to assess and intervene in pathological situations involving hypercapnia. The extensive conservation of innate immune and other biologically important cellular pathways between *Drosophila* and vertebrates, and the findings presented in this report, establish adult *Drosophila* and *Drosophila* S2 cells as genetically and molecularly tractable systems in which to identify, and define the functions of, components of non-neuronal CO_2 response pathways.

Materials and Methods

CO_2 exposure. CO_2 treatments on flies and cells were performed in a BioSpherix C-Chamber (BioSpherix Ltd, Redfield, NY) fitted with a ProCO_2 regulator using 20% CO_2/ 21% O_2/ 59% N_2 gas input. CO_2 concentrations for *in vivo* assays were confirmed using a FYRITE gas analyzer with CO_2 Indicator (Bacharach Inc., New Kensington, PA).

For cell culture experiments, pCO_2 and pH of media were measured using a STAT PROFILE pHOx Plus blood gas analyzer (Nova Biomedical, Waltham, MA). Culture medium was pre-equilibrated at desired CO_2 concentration overnight into which cells were then resuspended. Unless otherwise noted, cells were exposed to CO_2 for 5h prior to PGN challenge.

Cell culture, Western blotting and reagents. *Drosophila* S2 and S2* cells were grown in Schneider's insect medium (GIBCO, Carlsbad, CA, cat. #11720) with 10% FBS (Valley Biomedical, Winchester, VA, cat. #BS3032), supplemented with 0.2% Penicillin-Streptomycin (GIBCO, cat. #15140) and GlutaMAX (GIBCO, cat. #35050) at room temperature. S2 GFP-Relish cells were a gift from PH O'Farrell (UCSF). Mouse monoclonal anti-GFP antibody was used at 1:200 (Santa Cruz Biotechnology, Santa Cruz, CA, cat. #sc-9996). Anti-actin antibody from Sigma (cat. #A2066) was used at 1:2000. Priming of immune response in cell culture was achieved by treatment with 1mM final concentration 20-hydroxyecdysone (Sigma, St. Louis, MO, cat. #H5142) for 15h prior to exposure to CO_2 or other experimental condition (fresh ecdysone was added upon resuspension of cells in CO_2-pre-equlibrated medium). Purified *E. coli* peptidoglycan (*E. coli 0111:B4*, InvivoGen, San Diego, CA, cat. #tlrl-pgnec) was used at 100ng/mL final concentration for 5h (Fig.2D) or 2.5h (Figs. 2E, 4B,C, 5A,B). 1mM L-NAME (*Nw*-Nitro-L-arginine methyl ester hydrochloride, Sigma cat. #N5751) was added 10h before CO_2 treatment, 1mM SNAP (S-nitroso-N-acetyl-DL-penicillamine, Sigma cat. #N3398) was added 3h before CO_2 treatment. For pH adjustment of Schneider's medium, the indicated reagents (Fig. 5B) were added directly to the medium to the following final concentrations: 19mM MOPS (3-(N-morpholino)propanesulfonic acid, Sigma cat. #M-

8899), 25mM NaCl, 12.5mM HEPES (free acid, Cellgro cat. #25-060-Cl, Manassas, VA), 25mM NaOH (pre-equilibrated in CO_2 overnight before experiment). pH of solutions remained constant for the duration of treatment of cells.

Cell surface protein biotinylation assay. Surface biotinylation was performed as previously described (93). In brief, after treatment for 1h in indicated CO_2 conditions (Fig. 1G), S2 cells were labeled for 15min using 1 mg/ml EZ-link NHS-SS-biotin (Pierce Chemical Co. cat. #21331, Rockford, IL). Cells were then washed, lysed and 40mg of protein as measured by Bradford assay per sample were incubated overnight at 4°C with end-over-end shaking in the presence of streptavidin beads (Pierce Chemical Co.). The beads were thoroughly washed, resuspended in Laemmli sample buffer solution and loaded onto SDS-PAGE gel with 30mg total cell lysate. a5 anti-Na,K-ATPase antibody was obtained from the Developmental Studies Hybridoma Bank (U. of Iowa, IA) and used at 1:100 dilution.

Bacterial infection protocol. Fly stocks were raised on standard cornmeal-agar medium at 25°C. Batches of 25-30 CO_2-anesthetized (for <10 min) Oregon-R flies were challenged, in triplicate using a blinded protocol, by septic injury in the dorsal thorax with a sharpened tungsten needle previously dipped in a PBS solution containing the bacteria of interest. The vials were then exposed to CO_2 as described above at room temperature and the surviving flies counted at indicated intervals. *S. aureus* and *E. faecalis* (87) were a gift from DS Schneider (Stanford). All bacteria were grown on LB. Kaplan-Meier survival plots were generated from combining the triplicates for a total of ~75 flies per survival curve.

Drosophila developmental and fecundity assays. Developmental defects were assessed in embryos expressing GFP in the tracheal system (*btl*-Gal4 UAS-GFP/+) that were collected in air for 2h, transferred to experimental chambers containing air or elevated CO_2 for 19h and then evaluated for phenotypes. Defects were scored as moderate if embryos had 5 or fewer dorsal trunk breaks, and severe if there were more than 5 breaks. No embryos cultured in 13% CO_2 or ambient air displayed severe defects, and the frequency of moderate defects was 20% and 4%, respectively. For the egg hatching assay, eggs laid by flies in ambient air were collected on grape juice plates covered with yeast for 1-2 hours. The eggs from 3 separate experiments of at least 60 eggs each were then counted and transferred to various CO_2 conditions. 24 and 48h later, the hatched and unhatched eggs were counted. *Gr63a*^{1} mutants were a gift from L Vosshall (Rockefeller University). Fecundity was determined as per the protocol of Wang *et al.* (Wang, H.D. *et al.*, *PNAS* 101:12610-12615). In brief, 20 age-matched females and males were mated for 2 days in air at 25°C. The females were then transferred to the experimental conditions and eggs collected at approximately 8h intervals on standard yeasted grape juice plates. Each experiment was done in triplicate.

Quantitative PCR. 10mg of Trizol (Invitrogen, Carlsbad, CA, cat. #15596) extracted mRNA was treated with DNA-free (Ambion, Austin, TX, cat. #1906) according to manufacturer's directions. 1mg of DNA-free-treated mRNA was used in reverse-transcription reaction using Bio-Rad's iScript cDNA Synthesis Kit (Hercules, CA, cat. #170-8891). The cDNAs were diluted in water to ~1ng/ml. PCR reactions were performed using iQ SYBR Green Supermix from Bio-Rad (cat. #170-8882) according to manufacturer's directions. Real-time PCR was performed in 96-well plates on an iCycler

iQ (Bio-Rad). PCR conditions were: preincubation at 95°C for 3 min, 40 cycles: 30 sec at 95°C, 30 sec minute at 58°C, and 30 sec at 72°C. Quantitative analysis was performed using the iCycler iQ Optical System Software v3.0a. PCR reactions were performed in triplicate. The levels of expression of the gene of interest were normalized against ribosomal protein 49 (RP49) transcript levels in each sample. Primers used were as follows: RP49: forward 5'-GACGCTTCAAGGGACAGTATCTG-3', reverse 5'-AAACGCGGTTCTGCATGAG-3' (Gottar, M. *et al.*, *Nature* 416:640-644),

Drosomycin (Drm): forward 5'-CGTGAGAACCTTTTCCAATATGATG-3',

Reverse 5'TCCCAGGACCACCAGCAT-3';

Diptericin (Dpt): forward 5'-GCTGCGCAATCGCTTCTACT-3',

reverse 5'-TGGTGGAGTGGGCTTCATG-3' (Gobert, V. *et al.*, *Science (New York, N.Y* 302:2126-2130);

Attacin (Att): forward 5'-CTGACCAAGGGCATTGGCAATC-3',

reverse 5'-CTCCGGGCGTGTGTGTTTTGGTC-3';

Cecropin (Cec): forward 5'-CCATGAACTTCTACAACATCTTC-3',

reverse 5'-GCGATTCCCAGTCCCTGGATTG-3';

Metchnikowin (Mtk): forward 5'-GTGTGATGGCCACGGCTACATC-3',

reverse 5'-CGACATCAGCAGTGTGAATTTC-3';

Drosocin (Drs): forward 5'-CGCCTAAAGATGTGTGCATAC-3',

reverse 5'-CTCATTGTGTCACAATTGATTG-3';

Defensin (Def): forward 5'-CATGTCCTGGTGCATGAGGATG-3',

reverse: 5'-CGTTGCAGTAGCCGCCTTTGAAC-3'.

Whole fly microarrays. RNA was extracted from a minimum of 30 flies per condition using Trizol according to manufacturer's instructions. Microarray analysis was performed as previously described (Liu, G. *et al.*, *Physiological genomics* 25:134-141).

Bridge to Chapter V

In Chapters II-IV, I discussed studies in which genetic approaches were utilized to study physiological stress responses, making use of mutant *Drosophila* strains. Chapter VI describes a technique I have developed that makes the characterization of mutants such as these much faster and easier than is possible with current methodology.

CHAPTER V

GENOMIC REGIONAL CAPTURE FOR NEXT GENERATION SEQUENCING

In recent years, enormous leaps have been made in DNA sequencing technology, enabling researchers to collect immense amounts of sequence data in much less time and at a lesser cost than has previously been possible (100) (101). Despite the low cost and high throughput of these next generation sequencing (NGS) approaches, when seeking to locate the genomic identities of uncharacterized mutations it is still not feasible to sequence entire higher eukaryotic genomes. This fact necessitates a means by which smaller genomic regions of interest can be isolated for in depth analysis.

Traditionally, DNA polymerase chain reaction (PCR) has been the technique researchers have turned to for targeted enrichment of a particular genomic region. The upper size limit of products that PCR can reliably generate (5-50 kilobases (kb)) is considerably smaller than the genomic intervals typically identified by classical genetic techniques as containing mutations of interest however, and is orders of magnitude smaller than the amount of sequence data that can be generated in a single NGS run (up to 420 megabases (mb) at 6x coverage). The inadequacy of PCR for isolating large

genomic regions for NGS has led to the development of a number of new techniques designed to enrich for genomic regions that are hundreds or thousands of kb in size.

Recently, two separate research groups described techniques by which large regions of a target genome can be captured for NGS by hybridization of target DNA to custom DNA microarrays(26) (25). These approaches have been used to successfully capture regions as large as 5 mb. Despite their effectivenes, array based genomic regional capture approaches have some drawbacks. For one, complete sequence data must be available for the genome being captured in order to design the custom oligonucleotide probes contained on the array. These oligo sequences must also be carefully optimized to have highly similar melting temperatures, which can be a laborious process (26). Finally, custom high-density arrays are expensive, making the design of a new array for each new genomic region of interest impractical for smaller laboratories attempting to characterize mutants from genetic screens.

Other hybridization-based strategies have been used to enrich for specific sequences within larger complex DNA samples. Hybridization of DNA prepared from mixed bacterial populations to biotinylated oligonucleotide probes followed by capture with streptavidin-conjugated beads has been used to enrich for and identify species-specific sequences in both clinical and environmental microbiological samples (102) (103). Another approach based on hybridization of biotinylated bacterial artificial chromosome (BAC) DNA to homologous genomic DNA target regions of interest has been shown to be an effective strategy for resequencing large segments of human DNA by traditional Sanger DNA sequencing techniques (104). None of these

biotin/streptavidin-based approaches have been utilized to target genomic regions for sequencing by NGS, however.

In this chapter, I describe a method that I developed for isolating large genomic regions of interest for NGS. My technique involves the hybridization of sheared target genomic DNA to biotinylated homologous fosmid DNA. Following hybridization, biotinylated probe / target genomic DNA hybrids are captured with streptavidin-conjugated paramagnetic beads, and the target genomic DNA is eluted by heat denaturation. The eluted DNA is then amplified and sequenced using Solexa massively parallel sequencing. I have used this protocol to isolate a 336 kb genomic region that was determined to contain a mutation of interest from a *Caenorhabditis elegans* strain identified in a genetic screen. This captured DNA was sequenced using a fraction of a lane in an Illumina Genome Analyzer II (GA-II) Solexa instrument, resulting in 863,420 reads of 31 bases each that aligned to the *C. elegans genome,* 31% of which were from the targeted region. This represents 8,317,486 bases of sequence information from the 336 kb region of interest (~24x average coverage).

Materials and Methods

Genomic target DNA preparation. 5μg of *C. elegans* genomic DNA was sheared to an average size of 500 bp by sonication in a Bioruptor (Diagenode). The ends of the sheared DNA fragments were then blunted using a QuickBlunt kit (Invitrogen), following which, the fragments were purified with a PCR purification kit (Qiagen). A-overhangs were then added to the genomic fragments by incubation of the purified, blunted DNA with 150 units of Klenow DNA polymerase exo- (New England Biolabs) and dATP at

37°C for 30 minutes. The fragments were then purified with a mini-elute PCR purification kit (Qiagen). 7μL of 200 μM modified Solexa sequencing adapters (Top strand:

5'AATGATACGGCGACCACCGAGATCTACACTCTTTCCCTACACGACGCTCTT CCGATCTxxxxT 3'

Bottom strand:

5' phosphate xxxxAGATCGGAAGAGCTCGTATGCCGTCTTCTGCTTGC 3'(x – barcode bases),

were then ligated the sheared genomic fragments at 16°C for 2 hours using 2000 units of T4 DNA ligase (New England Biolabs). The ligation reaction was size separated by agarose gel electrophoresis, and fragments between 150-500 bp in size were purified from the gel using a Gel Extraction kit (Qiagen). The purified ligation products were then PCR amplified using Phusion high fidelity DNA polymerase (New England Biolabs) and the Solexa amplification primers

P5: 5'AATGATACGGCGACCACCGA3' and

P7: 5'CAAGCAGAAGACGGCATACGA3'. The following cycling conditions were used for PCR: 98°C for 2 minutes, 15 cycles of 98°C for 10 seconds, 65°C for 30 sec, 72°C for 15 seconds. Following amplification, samples were size separated by agarose gel electrophoresis, and fragments between 150 and 500 bp were purified with a Gel extraction kit (Qiagen).

Biotinylated probe preparation. 11 fosmids which, taken together, are homologous to a 336 kb region of the *C. elegans* genome, were pooled in equal amounts. 100 ng of this mixture were combined with 20 μL of 2.5x random octamer solution

(Invitrogen) and heated to 100°C for 5 minutes. The mixture was rapidly cooled in an ice/water bath, following which 5 μL of biotin dNTP mixture (1mM biotin-14-dCTP, 1mM dCTP, 2mMdATP, 2mM dGTP, 2 mM dGTP, in 10 mM Tris-HCl (pH 7.5), 1mM Na_2EDTA) (Invitrogen) was added, along with 1 μL of Klenow fragment DNA polymerase (Invitrogen) and ultra pure water to bring the reaction volume to 50 μL. The reaction was then incubated at 37°C for 1 hour, following which, the products were size-separated on an agarose gel, and the predominant 100 bp product was purified with a Gel extraction kit (Qiagen).

Streptavidin bead preparation. 50 μL of M270 streptavidin Dynabeads (Invitrogen) were washed 3 times with 100 μL of 6x SSC and resuspended in 100 μL of bead block buffer (2% I-Block (Tropix), 0.5% SDS, 1x PBS) (105). Beads were incubated at room temperature for 30 minutes with occasional mixing, and were then magnetically captured, and washed 3x with 6x SSC.

Hybridization, immobilization, elution and sequencing. 5 μg of adapted, purified genomic DNA was combined with 150 ng of purified biotinylated probe in 300 μL of hybridization buffer (54% formamide, 1x SSC, 1% SDS, 5.4x Denhardt's solution (Sigma), 1mg/ml Salmon sperm DNA (Invitrogen). The mixture was heated to 100°C for 2 minutes, then transferred to a 42°C incubator, where it was incubated with mixing overnight. Following overnight incubation, biotinylated probe/genomic DNA fragment hybrids were immobilized by binding to prepared blocked and washed streptavidin beads by combining the hybridization mixture (300 μL) with the bead/SSC mixture (100 μL), and incubating at room temperature for 15 minutes with occasional mixing. Beads were

then magnetically captured, and washed 3x with wash solution 1 (1x SSC, 0.15% SDS), 3x with wash solution 2 (.2x SSC), and 3x with wash solution 3 (0.05x SSC). After the final wash step, the beads were resuspended in 200 μL of ultra pure water, and heated to 100°C for 2 minutes, and quickly magnetically captured. The supernatant was carefully collected and concentrated to a volume of 20 μL in a speedvac concentrator (Savant). 10μL of the concentrated supernatant was then used as template for a PCR reaction utilizing Solexa P5 and P7 primers and Phusion high fidelity DNA polymerase (New England Biolabs) (2 minutes 98°C, 24 cycles of 98°C for 10 seconds, 65°C for 30 sec, 72°C for 15 seconds). The PCR product was purified with a PCR cleanup kit (Qiagen), quantified, and submitted for Solexa sequencing on an Illumina Genome Analyzer II.

Results

Sequencing targeted genomic regions by NGS has previously been an expensive proposition requiring the design and manufacture of custom DNA microarrays. The method described here is considerably cheaper, easier, and faster than existing techniques because readily available fosmid clones are used as the capture probe in place of the microarrayed custom oligonucleotides (Figure 1). In this pilot experiment, DNA from 11 fosmid clones representing 336,224 bases of the *C. elegans* were combined and used as the capture probe (Table 1). The addition of biotin to the probe DNA allowed the subsequent capture of hybridized target fragments using streptavidin-conjugated paramagnetic beads. Biotin addition was carried out by the replication of the probe DNA from random primers in the presence of biotinylated nucleotides. The extremely high

affinity of the biotin-streptavidin bond allowed stringent washing of the beads to minimize the isolation of non-target DNA.

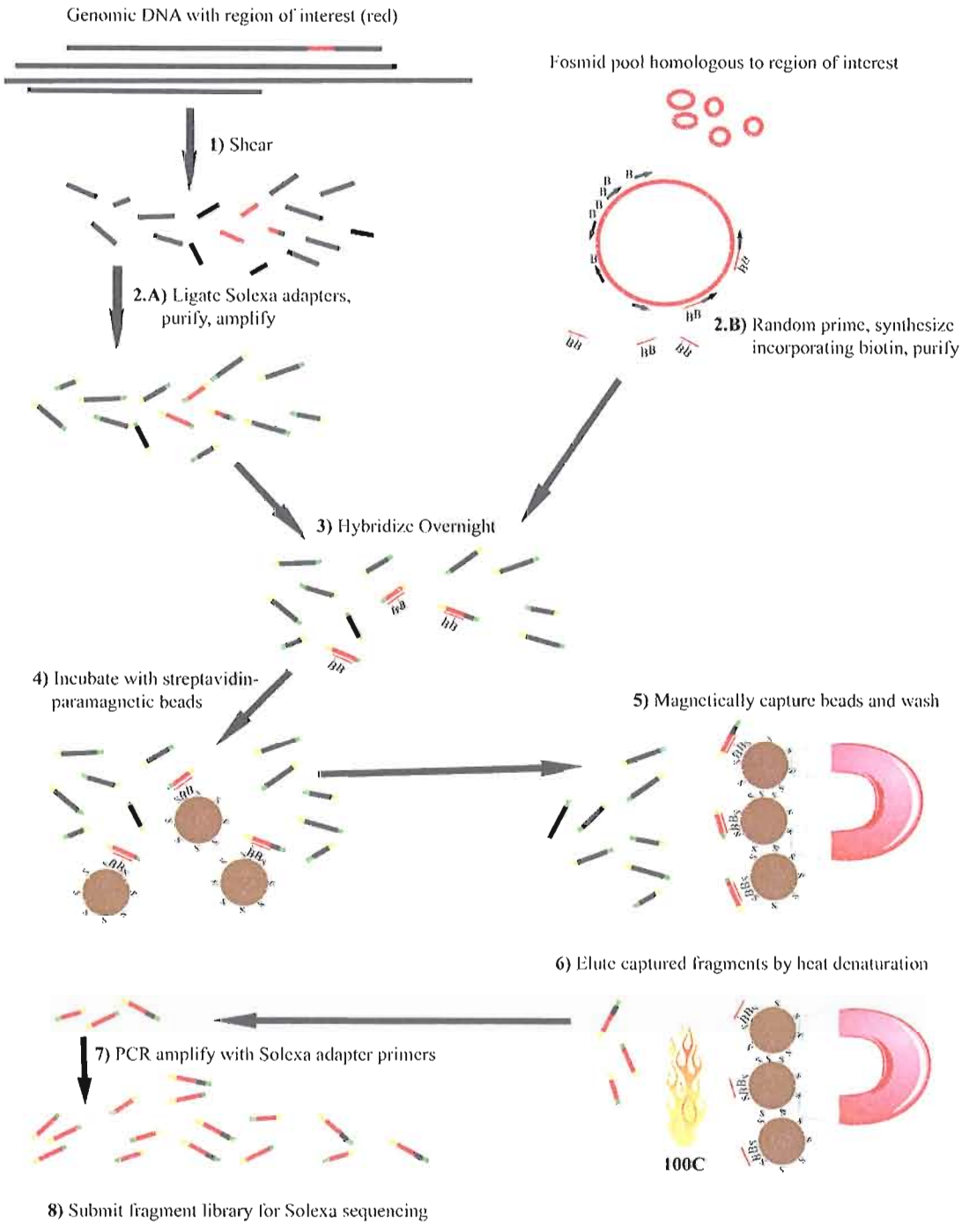

Figure 1. Schematic representation of regional capture protocol. Genomic DNA containing a region of interest is (1) sheared, and Solexa adapters are added by ligation and amplification (2.A). A pool of Fosmids which is homologous to the region of interest is (2.B) converted to biotinylated probe by Klenow polymerase-mediated synthesis incorporating biotinylated nucleotides. Sheared genomic DNA and biotinylated probe are hybridized (3), and the probe/target DNA hybrids are by the addition of streptavidin paramagnetic beads (4), which are magnetically captured and washed (5). Genomic target fragments are then eluted by heat denaturation (6), and amplified by PCR with adapter-specific primers (7). The library of target region DNA fragments is then submitted for Solexa sequencing.

Table 1. Fosmid clones used for preparation of biotinylated probes. The genomic coordinates of the fosmids are listed. Taken together, these fosmids cover a genomic region of 336,224 bases.

Fosmid clone	Chromosome	Clone start	Clone stop
WRM0613cF02	V	14251674	14290493
WRM0610dB09	V	14270881	14304812
WRM0629dD01	V	14301880	14332947
WRM0619aC10	V	14322557	14352744
WRM0636cG07	V	14367151	14399508
WRM0617aH02	V	14385040	14425855
WRM0630cB06	V	14420643	14460182
WRM0634aD11	V	14453407	14491275
WRM0627aC04	V	14504084	14537563
WRM061aB03	V	14522269	14560418
WRM0615aE07	V	14558577	14587898

Five μg of genomic target DNA was used as starting material. This DNA was sheared and asymmetric Solexa sequencing adapters were attached by ligation. Following ligation, the reaction was gel extracted to select the appropriate fragment size for Solexa sequencing, as well as to remove adapter dimers. The fragments were then amplified by PCR using an extremely high fidelity polymerase. The sheared, adapted genomic target DNA was then hybridized overnight to the previously biotinylated fosmid DNA. After hybridization, target DNA/biotinylated fosmid DNA hybrids were purified using streptavidin beads, which were stringently washed to remove un-hybridized background DNA. Finally, the captured genomic DNA was eluted from the beads by heat denaturation, and PCR amplified. After a final purification, the DNA sample was ready to be Solexa sequenced. This entire protocol, excluding sequencing, can be completed in two days.

Prior to submitting samples for NGS, I cloned several fragments in the library and sequenced the inserts using Sanger sequencing (Figure 2A). This allowed me to verify that the Solexa amplification and sequencing primers would bind in the proper locations

for NGS, and verified that many of the clones contained DNA that aligns to the *C. elegans* genome in the target region. In order to provide additional verification of enrichment of the target genomic region in the purified samples, I designed two sets of PCR primers to amplify sequences within the captured DNA area (Figure 2B). Equal quantities of pre-hybridization input DNA and purified DNA were used as template for PCR. This reaction showed significant enrichment of the targeted region in the purified sample.

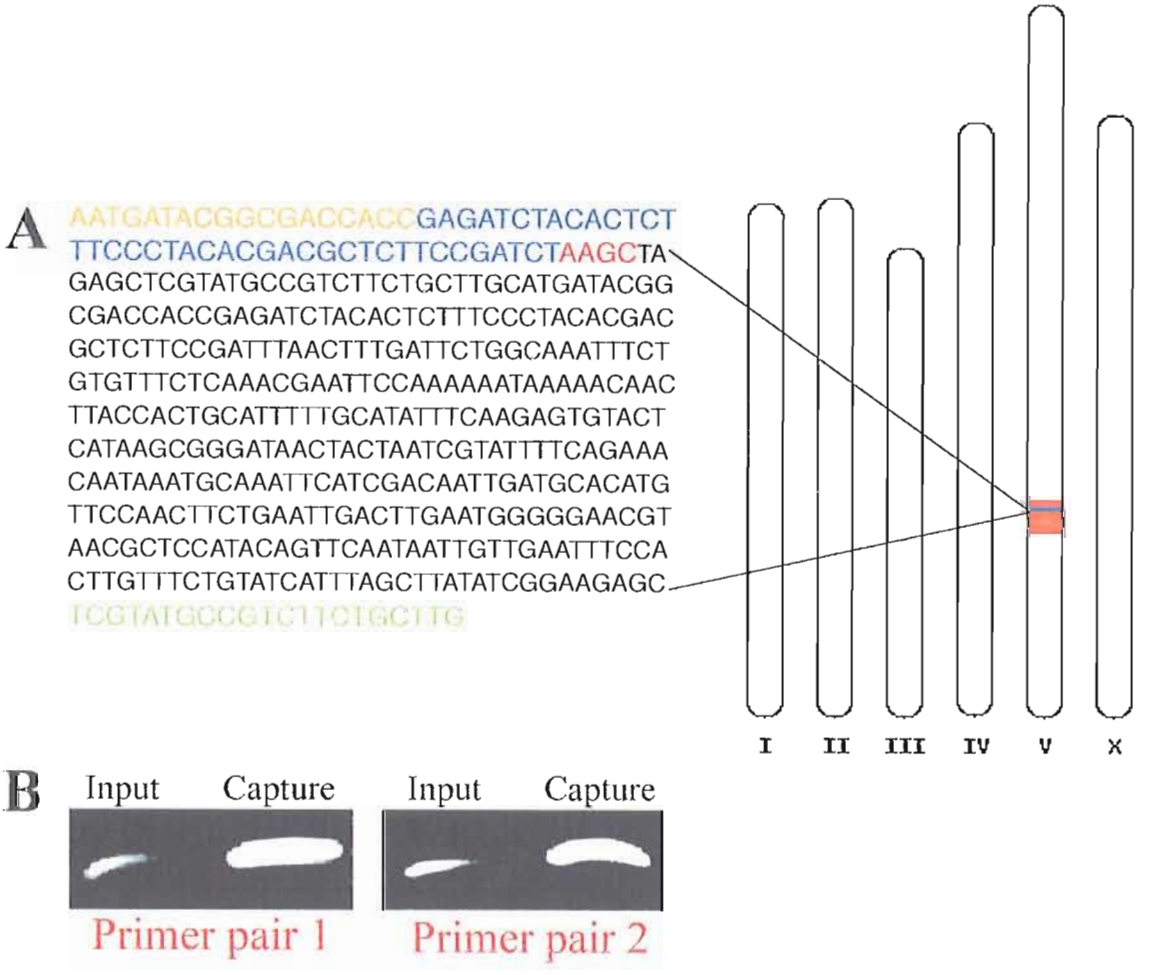

Figure 2. Verification of captured library prior to NGS. Before submitting the captured library of fragments for Solexa sequencing, fragments were cloned and sequenced. A) An example clone sequence shows the correct Solexa P5 (orange) and P7 (green) amplification primer sequences, Solexa sequencing primer sequence (blue), barcode (red), and an insert sequence that aligns to the target region of the *C. elegans* genome (highlighted in red) by BLAST. B) Equal amounts of input and region-captured DNA fragments were used as template for PCR using two primer sets that amplify products within the target region. Much more product is generated using the captured template indicating enrichment of the target region.

Because barcoded Solexa adapters were used in the preparation of the DNA sample, samples prepared with other barcodes by other researchers could be combined with my sample in the same lane of the GA-II so that the cost of the sequencing run could

be shared. The GA-II data analysis software aligns the output of the sequencing run to available reference genomes. This alignment yielded 863,420 reads of 31 bases each that aligned to unique locations in the *C. elegans* genome. Of these reads, 268,305 (31%) were from within the targeted region. These reads provide 8,317,455 bases of data, which provides an average 24x coverage of the targeted region (Figure 3). The variability in coverage at different locations within the region may be related to GC content variations within the region, or could be related to the number of cycles used in the amplification reactions in the protocol. Future optimization of the protocol will probably be able to provide more consistent depth of coverage throughout the captured region.

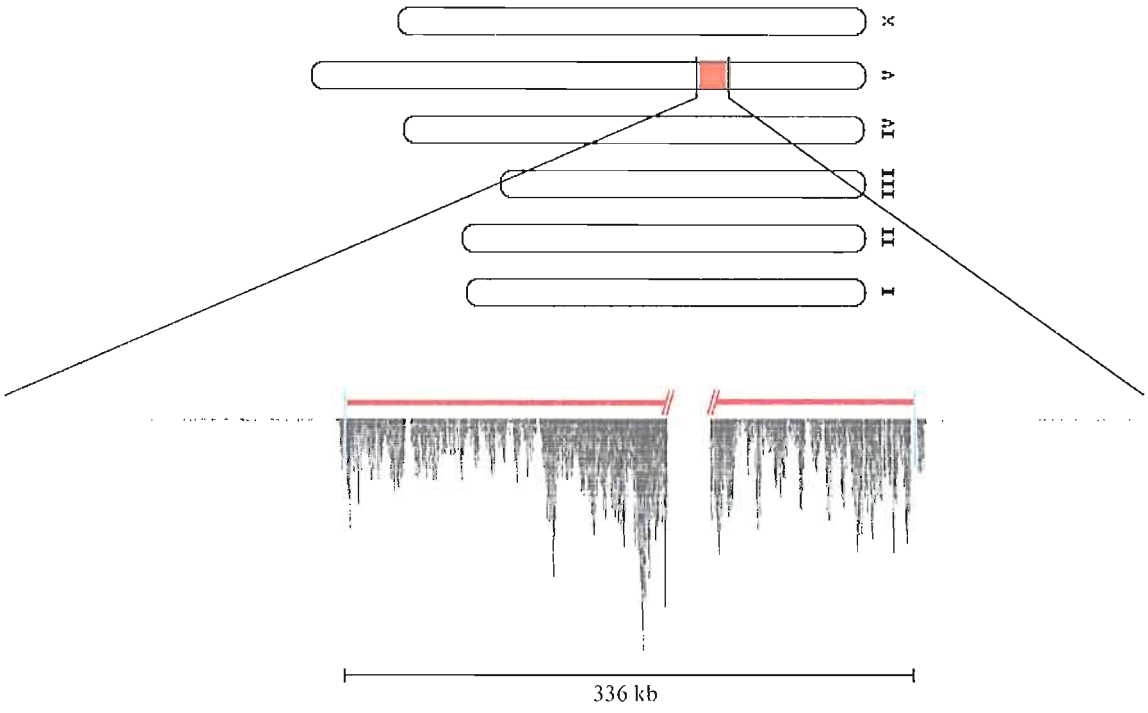

Figure 3. Graphical representation of sequences from regionally captured samples aligned to a portion of the *C. elegans* genome. The area of chromosome V that was targeted for capture is indicated in red bordered by blue lines. Black bars beneath the zoomed in area of chromosome V indicate sequence reads. 31% of the total sequence reads that aligned uniquely to the genome were within the target region. Other reads were scattered randomly throughout the genome.

Discussion

One major drawback of NGS approaches is that they do not provide an easy means of sequencing specific genomic areas since the sequencing reaction does not proceed from a fixed gene-specific primer as it does in Sanger sequencing. Because of this limitation, a method for capturing specific genomic regions for NGS by DNA microarray hybridization was previously developed. Here, I have described an alternative to the array-based capture method, which is cheaper, faster, and easier to perform.

I have demonstrated the effectiveness of this protocol by capturing and sequencing a 336 kb region of the *C. elegans* genome from a mutant strain isolated in a genetic screen. Despite the fact that a large number of sequences obtained were from outside the region of interest, the enrichment was sufficient to sequence the mutation-containing region with an average 24x coverage. The data from the sequencing run was obtained quite recently, so we have only begun to analyze the data. In fairly short order, we will be able to visualize SNPs between the obtained aligned sequences and the *C. elegans* reference genome, which should make identification of the SNP responsible for the mutant phenotype quite easy.

This regional capture technique has applications beyond the characterization of mutants from genetic screens in model organisms. Using a fraction of a lane in a GA-II NGS instrument, my protocol was able to provide 24x coverage of the targeted region. This depth of coverage would have increased substantially if the entire lane had been dedicated to sequencing the captured region. With increased depth of coverage, the captured region could be assembled without the aid of a reference genome, and this protocol would be a viable method of capturing and sequencing genomic regions of non-model organisms with incompletely sequenced genomes. A variation on this protocol is currently being evaluated as a means of mapping transposon insertion sites in maize. Indeed, researchers should be able to make use of this protocol, or a modification of it, for any situation in which they would like to enrich for a specific genomic location for NGS.

Bridge to Chapter VI

In Chapter V I described a technique I have developed for sequencing specific DNA regions using NGS. This protocol is considerably faster and less expensive than existing techniques. In Chapter VI I will summarize the findings from Chapters II, III, IV, and V, and highlight the broader significance of these results

CHAPTER VI

CONCLUSION

Stress-responsive gene regulation

A key adaptation organisms make in order to survive physiological stresses is the differential regulation of gene expression. This regulation is directly carried out by stress-responsive transcription factors. One physiological stress that all eukaryotic organisms must cope with is hypoxia. In Chapter II I have identified genes that are regulated by hypoxia, and have determined the roles of five different hypoxia-responsive transcription factors in the regulation of this set of hypoxia-modulated transcripts. This was achieved by examining hypoxic gene expression in *D. melanogaster* mutants lacking the hypoxia-responsive transcription factors *HIF-1, FOXO, Rel, p53*, and *MTF-1*, and by refining the lists of affected transcripts using bioinformatic analysis. I have identified several previously characterized target genes of the five hypoxia-responsive transcription factors, as well as genes that have never been previously described as targets. I have also identified a mechanism by which HIF-1 can contribute to the activation of FOXO during hypoxia through the HIF-1-dependent transcriptional up regulation of *Imp-L2*. Finally, I

have determined that FOXO plays a much larger role in hypoxic gene regulation than has previously been thought.

One set of genes that are highly transcriptionally up regulated in response to hypoxia are those encoding heat shock proteins. In Chapter III, we showed that HIF-1 plays a significant role in the transcriptional up regulation of *Heat shock protein (HSP)* genes during hypoxia. This occurs because HIF-1 directly up regulates the transcription of the *Heat shock factor (HSF)* gene during hypoxia, and this up regulation is necessary for the full transcriptional induction of *HSP*'s. We showed that this HIF-1-dependent up-regulation of *HSF* during hypoxia is functionally significant because flies with reduced HSF levels during hypoxia are less viable than wild-type flies.

Exposure to elevated CO_2 levels (hypercapnia) is another stress that eukaryotes adapt to by modulating gene expression. In Chapter IV, we identified genes that are differentially regulated during hypercapnia in *Drosophila*. We found that the transcription of immune response genes that are known targets of the transcription factor Relish (Rel) is significantly repressed by hypercapnia. Interestingly, we showed that this transcriptional repression occurs by a pathway that is either downstream or in parallel to the canonical Rel activation pathway. Our results have medical relevance because hypercapnia is frequently experienced by patients suffering from chronic pulmonary obstructive disease and the suppression of immune response genes may promote bacterial infections in patients experiencing this physiological stress. This study also establishes *Drosophila* as a powerful model system for the study of hypercapnia.

Regional capture for next generation sequencing

The Sanger method of DNA sequencing is a well-established technology that is widely available to researchers at numerous institutions across the world. However, the amount of sequence data produced per Sanger sequencing run is limited to less than 1000 bases, making sequencing large DNA fragments with this technology costly and slow. To address this limitation, next generation sequencing (NGS) techniques have been developed in recent years that produce much more sequence data per run. The downside of these new approaches is that the sequence reads produced by NGS instruments are not targeted to a specific region of the template DNA making the sequencing of specific regions of complex genomic DNA samples impossible with these techniques. Custom DNA microarray-based regional capture schemes have been developed to facilitate the enrichment of specific DNA regions for NGS, but these approaches are slow and costly. In Chapter V I have described a regional capture protocol that provides enrichment of target DNA sequences that is comparable to the array-based schemes. My approach is considerably faster and less expensive, however because biotinylated fosmid DNA is used in place of custom DNA microarrays as the probe for the hybridization-based capture. I have demonstrated the effectiveness of my protocol by capturing a genomic DNA region from a *C. elegans* strain that contains a mutation causing SNP. Sequencing this region by NGS provided an average of 24x coverage for every base in the targeted region, which was more than sufficient for identifying the SNP. My regional capture protocol is broadly applicable to any situation in which a researcher desires to enrich for a specific region of a complex DNA sample for sequencing by NGS.

APPENDIX

ONLINE SUPPLEMENTAL MATERIAL FOR CHAPTER IV

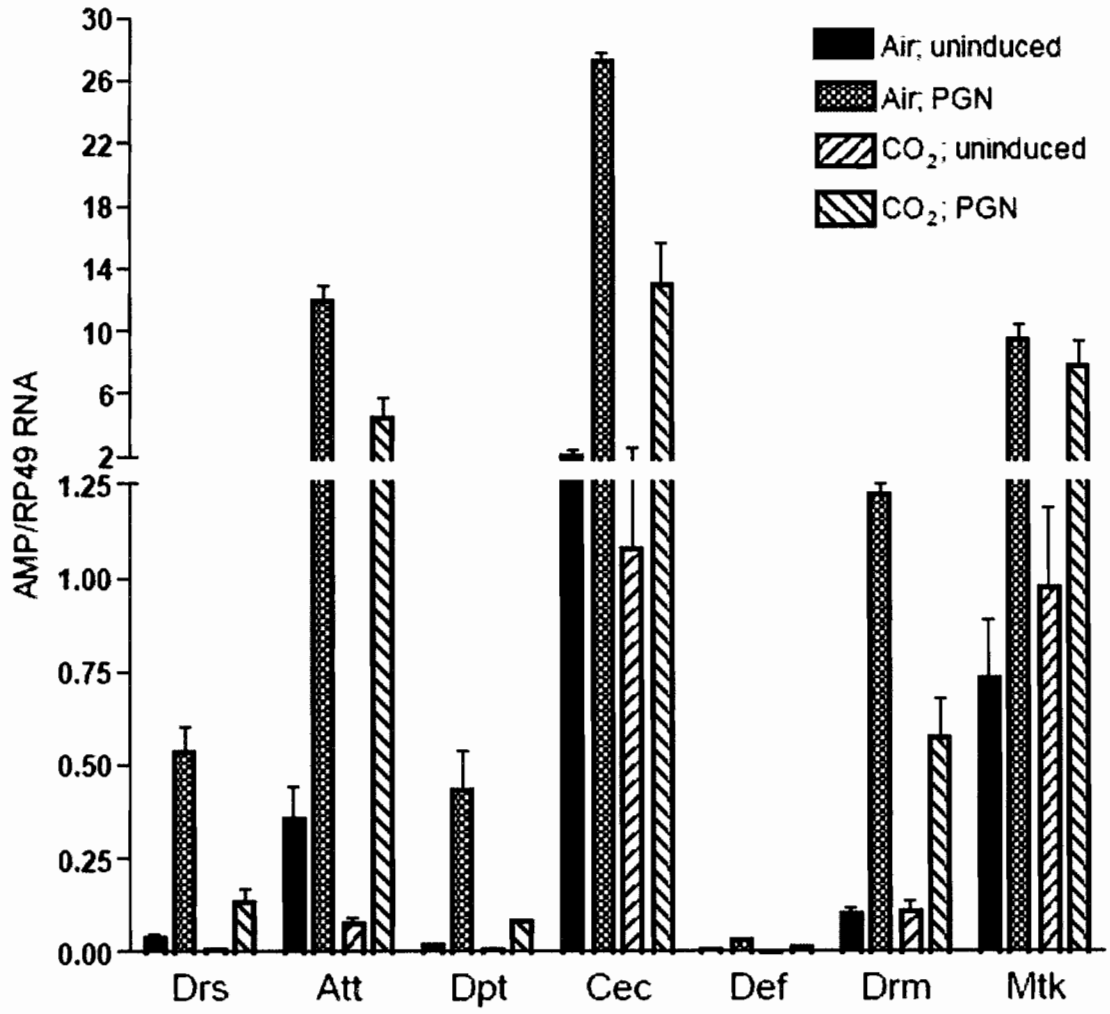

Figure S1. Absolute levels of antimicrobial peptide RNAs in S2* cells, normalized to RP49. CO_2 = 13%, 10h duration before RNA extraction; PGN = 5h before RNA extraction. This is the same experiment as in Figure 2C and D. AMP abbreviations are as in Figure 2.

Table S1. Hypercapnia strongly down-regulates egg formation genes, but does not up-regulate genes induced by hypoxic, heat shock, or oxidative stress responses.

A. Egg formation genes	Fold induction 13% CO_2	C. Heat shock-induced genes[¶]	Fold induction 13% CO_2
CG6517 Chorion protein 18	-42.3	CG16749	1
CG6524 Chorion protein 19	-38.5	CG18493	1.1
CG6533 Chorion protein 16	-28.1	CG9470 Metallothionein A	1
CG11213 Chorion protein 38	-26.5	CG3106	-1
CG1778 Chorion protein 36	-20	CG6730 Cyp4d21	-1.2
CG6519 Chorion protein 15	-10.4	CG1946	1
CG2175 Defective chorion 1	-9.8	CG9080	-1.1
CG9271 Vitelline membrane 34Ca	-7.2	CG6602	-1.1
CG9048 Vitelline membrane 26Aa	-5.9	CG3360 Cyp313a1	-1.1
CG15349 Chorion protein a	-5.8	CG13833 (up 2.9-fold in heat shock)	1.1
CG15351 Chorion protein c	-4.8		
CG9046 Vitelline membrane 26Ab	-4		

B. Hypoxia-induced genes[§]		D. Oxidative stress-induced genes[†]	
CG11765 Peroxiredoxin	-1.2	CG4533 l(2)efl	-1.2
CG11949 Coracle	-1.3	CG5164 GstE1	1
CG12896	1.1	CG10794 Diptericin B	-1.4
CG10160 ImpL3	1	CG31628 ade3	-1
CG6494 Hairy h	-1.3	CG18466 Nmdmc	1.1
CG13499	-1.1	CG7632	-1.1
CG32130	-1.2	CG10146 Attacin A	-2.3
CG10078 Phosphoribosylamidotransferase 2	-1.6	CG8772 nemy	1
CG1600	1.1	CG14121	-1
CG8846 Thor	1.2	CG1383 Defensin	-2.1

Average fold induction in 13% CO_2 (24h, CO_2 versus air) of genes specific for egg formation (A) and selected genes reported to be highly induced by previously characterized stresses (B-D). Fold induction is the average of 3 separate microarray experiments of 5-day old flies. Stress genes are shown in decreasing order of induction magnitude for particular stresses with maximal and minimal values shown in parentheses. See references below for fold up-regulation by hypoxia[§] (range: CG8846 Thor 4.7-fold to CG11765 Peroxiredoxin 8.4-fold), heat shock[¶] (range: CG13833 2.9-fold to CG16749 41-fold) and oxidative stress[†] (range: CG1383 Defensin 1.6-fold to CG4533 l(2)efl 7-fold).

[§]Hypoxia-induced genes reported by G. Liu *et al.*, Physiol. Genomics 25: 131-141, 2006

[¶]Heat shock-induced genes reported by J.G. Sorensen *et al.*, Cell Stress & Chaperones, (2005) 10 (4) 312-328

[†]Oxidative stress-induced genes reported by G.N. Landis *et al.*, PNAS 2004;101(20):7663-8

Table S2. Hypercapnia does not affect cell viability. Trypan blue dye exclusion assay performed with S2* cells shows that hypercapnia and the other experimental conditions used do not significantly alter cell viability. If indicated, cells were primed for immune response with 20-hydroxyecdysone (ecd) at 0h, placed in 13% CO_2 at 15h, and/or stimulated with *E. coli* PGN at 20h. Rapid cell death by strong oxidative stress shown for comparison.
[†]standard deviation of triplicate experiments in parentheses.

Experimental condition	Time at measurement (h)	% cells containing dye[†]
Air	0	6.9 (0.13)
Air	23	5.6 (0.74)
Air + ecd	15	5.6 (0.82)
Air + ecd	23	4.4 (1.07)
13% CO_2 + ecd	23	5.7 (1.30)
air + ecd + PGN	23	5.2 (1.54)
13% CO_2 + ecd + PGN	23	6.0 (0.98)
Air + 100mM t-butyl hydroperoxide	1.5	31
Air + 1M t-butyl hydroperoxide	1.5	100

REFERENCES

1. Semenza, G.L. 2007. Hypoxia-inducible factor 1 (HIF-1) pathway. *Sci STKE.* 2007:cm8.

2. Kewley, R.J., M.L. Whitelaw, and A. Chapman-Smith. 2004. The mammalian basic helix-loop-helix/PAS family of transcriptional regulators. *Int J Biochem Cell Biol.* 36:189-204.

3. Wang, G.L., B.H. Jiang, E.A. Rue, and G.L. Semenza. 1995. Hypoxia-inducible factor 1 is a basic-helix-loop-helix-PAS heterodimer regulated by cellular O2 tension. *Proc Natl Acad Sci U S A.* 92:5510-5514.

4. Stockmann, C., and J. Fandrey. 2006. Hypoxia-induced erythropoietin production: a paradigm for oxygen-regulated gene expression. *Clin Exp Pharmacol Physiol.* 33:968-979.

5. Centanin, L., P.J. Ratcliffe, and P. Wappner. 2005. Reversion of lethality and growth defects in Fatiga oxygen-sensor mutant flies by loss of hypoxia-inducible factor-alpha/Sima. *EMBO Rep.* 6:1070-1075.

6. Baird, N.A., D.W. Turnbull, and E.A. Johnson. 2006. Induction of the heat shock pathway during hypoxia requires regulation of heat shock factor by hypoxia-inducible factor-1. *J Biol Chem.* 281:38675-38681.

7. Accili, D., and K.C. Arden. 2004. FoxOs at the crossroads of cellular metabolism, differentiation, and transformation. *Cell.* 117:421-426.

8. Brunet, A., L.B. Sweeney, J.F. Sturgill, K.F. Chua, P.L. Greer, Y. Lin, H. Tran, S.E. Ross, R. Mostoslavsky, H.Y. Cohen, L.S. Hu, H.L. Cheng, M.P. Jedrychowski, S.P. Gygi, D.A. Sinclair, F.W. Alt, and M.E. Greenberg. 2004. Stress-dependent regulation of FOXO transcription factors by the SIRT1 deacetylase. *Science.* 303:2011-2015.

9. Bakker, W.J., I.S. Harris, and T.W. Mak. 2007. FOXO3a is activated in response to hypoxic stress and inhibits HIF1-induced apoptosis via regulation of CITED2. *Mol Cell.* 28:941-953.

10. Chen, F., V. Castranova, X. Shi, and L.M. Demers. 1999. New insights into the role of nuclear factor-kappaB, a ubiquitous transcription factor in the initiation of diseases. *Clin Chem.* 45:7-17.

11. Minakhina, S., and R. Steward. 2006. Nuclear factor-kappa B pathways in Drosophila. *Oncogene.* 25:6749-6757.

12. Chandel, N.S., W.C. Trzyna, D.S. McClintock, and P.T. Schumacker. 2000. Role of oxidants in NF-kappa B activation and TNF-alpha gene transcription induced by hypoxia and endotoxin. *J Immunol.* 165:1013-1021.

13. Koong, A.C., E.Y. Chen, and A.J. Giaccia. 1994. Hypoxia causes the activation of nuclear factor kappa B through the phosphorylation of I kappa B alpha on tyrosine residues. *Cancer Res.* 54:1425-1430.

14. Wingrove, J.A., and P.H. O'Farrell. 1999. Nitric oxide contributes to behavioral, cellular, and developmental responses to low oxygen in Drosophila. *Cell.* 98:105-114.

15. Galkin, A., A. Higgs, and S. Moncada. 2007. Nitric oxide and hypoxia. *Essays Biochem.* 43:29-42.

16. Liu, G., J. Roy, and E.A. Johnson. 2006. Identification and function of hypoxia-response genes in Drosophila melanogaster. *Physiol Genomics.* 25:134-141.

17. Slee, E.A., D.J. O'Connor, and X. Lu. 2004. To die or not to die: how does p53 decide? *Oncogene.* 23:2809-2818.

18. Chen, D., M. Li, J. Luo, and W. Gu. 2003. Direct interactions between HIF-1 alpha and Mdm2 modulate p53 function. *J Biol Chem.* 278:13595-13598.

19. Chandel, N.S., M.G. Vander Heiden, C.B. Thompson, and P.T. Schumacker. 2000. Redox regulation of p53 during hypoxia. *Oncogene.* 19:3840-3848.

20. Li, Y., T. Kimura, J.H. Laity, and G.K. Andrews. 2006. The zinc-sensing mechanism of mouse MTF-1 involves linker peptides between the zinc fingers. *Mol Cell Biol.* 26:5580-5587.

21. Zhang, B., O. Georgiev, M. Hagmann, C. Gunes, M. Cramer, P. Faller, M. Vasak, and W. Schaffner. 2003. Activity of metal-responsive transcription factor 1 by toxic heavy metals and H2O2 in vitro is modulated by metallothionein. *Mol Cell Biol.* 23:8471-8485.

22. Green, C.J., P. Lichtlen, N.T. Huynh, M. Yanovsky, K.R. Laderoute, W. Schaffner, and B.J. Murphy. 2001. Placenta growth factor gene expression is induced by

hypoxia in fibroblasts: a central role for metal transcription factor-1. *Cancer Res.* 61:2696-2703.

23. Murphy, B.J., G.K. Andrews, D. Bittel, D.J. Discher, J. McCue, C.J. Green, M. Yanovsky, A. Giaccia, R.M. Sutherland, K.R. Laderoute, and K.A. Webster. 1999. Activation of metallothionein gene expression by hypoxia involves metal response elements and metal transcription factor-1. *Cancer Res.* 59:1315-1322.

24. Sanger, F., S. Nicklen, and A.R. Coulson. 1977. DNA sequencing with chain-terminating inhibitors. *Proc Natl Acad Sci U S A.* 74:5463-5467.

25. Okou, D.T., K.M. Steinberg, C. Middle, D.J. Cutler, T.J. Albert, and M.E. Zwick. 2007. Microarray-based genomic selection for high-throughput resequencing. *Nat Methods.* 4:907-909.

26. Albert, T.J., M.N. Molla, D.M. Muzny, L. Nazareth, D. Wheeler, X. Song, T.A. Richmond, C.M. Middle, M.J. Rodesch, C.J. Packard, G.M. Weinstock, and R.A. Gibbs. 2007. Direct selection of human genomic loci by microarray hybridization. *Nat Methods.* 4:903-905.

27. Brown, J.M., and A.J. Giaccia. 1998. The unique physiology of solid tumors: opportunities (and problems) for cancer therapy. *Cancer Res.* 58:1408-1416.

28. Hammond, E.M., and A.J. Giaccia. 2005. The role of p53 in hypoxia-induced apoptosis. *Biochem Biophys Res Commun.* 331:718-725.

29. Chung, M.J., C. Hogstrand, and S.J. Lee. 2006. Cytotoxicity of nitric oxide is alleviated by zinc-mediated expression of antioxidant genes. *Exp Biol Med (Maywood).* 231:1555-1563.

30. Bacon, N.C., P. Wappner, J.F. O'Rourke, S.M. Bartlett, B. Shilo, C.W. Pugh, and P.J. Ratcliffe. 1998. Regulation of the Drosophila bHLH-PAS protein Sima by hypoxia: functional evidence for homology with mammalian HIF-1 alpha. *Biochem Biophys Res Commun.* 249:811-816.

31. Lavista-Llanos, S., L. Centanin, M. Irisarri, D.M. Russo, J.M. Gleadle, S.N. Bocca, M. Muzzopappa, P.J. Ratcliffe, and P. Wappner. 2002. Control of the hypoxic response in Drosophila melanogaster by the basic helix-loop-helix PAS protein similar. *Mol Cell Biol.* 22:6842-6853.

32. Ishwaran, H., J.S. Rao, and U.B. Kogalur. 2006. BAMarraytrade mark: Java software for Bayesian analysis of variance for microarray data. *BMC Bioinformatics.* 7:59.

33. Honegger, B., M. Galic, K. Kohler, F. Wittwer, W. Brogiolo, E. Hafen, and H. Stocker. 2008. Imp-L2, a putative homolog of vertebrate IGF-binding protein 7, counteracts insulin signaling in Drosophila and is essential for starvation resistance. *J Biol.* 7:10.

34. Murphy, B.J., T. Kimura, B.G. Sato, Y. Shi, and G.K. Andrews. 2008. Metallothionein induction by hypoxia involves cooperative interactions between metal-responsive transcription factor-1 and hypoxia-inducible transcription factor-1alpha. *Mol Cancer Res.* 6:483-490.

35. Krieg, A.J., E.M. Hammond, and A.J. Giaccia. 2006. Functional analysis of p53 binding under differential stresses. *Mol Cell Biol.* 26:7030-7045.

36. Pear, W.S., and M.C. Simon. 2005. Lasting longer without oxygen: The influence of hypoxia on Notch signaling. *Cancer Cell.* 8:435-437.

37. Semenza, G.L. 1999. Regulation of mammalian O2 homeostasis by hypoxia-inducible factor 1. *Annu Rev Cell Dev Biol.* 15:551-578.

38. Hon, W.C., M.I. Wilson, K. Harlos, T.D. Claridge, C.J. Schofield, C.W. Pugh, P.H. Maxwell, P.J. Ratcliffe, D.I. Stuart, and E.Y. Jones. 2002. Structural basis for the recognition of hydroxyproline in HIF-1 alpha by pVHL. *Nature.* 417:975-978.

39. Huang, L.E., J. Gu, M. Schau, and H.F. Bunn. 1998. Regulation of hypoxia-inducible factor 1alpha is mediated by an O2-dependent degradation domain via the ubiquitin-proteasome pathway. *Proc Natl Acad Sci U S A.* 95:7987-7992.

40. Ivan, M., K. Kondo, H. Yang, W. Kim, J. Valiando, M. Ohh, A. Salic, J.M. Asara, W.S. Lane, and W.G.J. Kaelin. 2001. HIFalpha targeted for VHL-mediated destruction by proline hydroxylation: implications for O2 sensing. *Science.* 292:464-468.

41. Jaakkola, P., D.R. Mole, Y.M. Tian, M.I. Wilson, J. Gielbert, S.J. Gaskell, A. Kriegsheim, H.F. Hebestreit, M. Mukherji, C.J. Schofield, P.H. Maxwell, C.W. Pugh, and P.J. Ratcliffe. 2001. Targeting of HIF-alpha to the von Hippel-Lindau ubiquitylation complex by O2-regulated prolyl hydroxylation. *Science.* 292:468-472.

42. Huang, L.E., and H.F. Bunn. 2003. Hypoxia-inducible factor and its biomedical relevance. *J Biol Chem.* 278:19575-19578.

43. Pugh, C.W., and P.J. Ratcliffe. 2003. Regulation of angiogenesis by hypoxia: role of the HIF system. *Nat Med.* 9:677-684.

44. Vogelstein, B., and K.W. Kinzler. 2004. Cancer genes and the pathways they control. *Nat Med.* 10:789-799.

45. Semenza, G.L. 2002. HIF-1 and tumor progression: pathophysiology and therapeutics. *Trends Mol Med.* 8:S62-7.

46. Pouyssegur, J., F. Dayan, and N.M. Mazure. 2006. Hypoxia signalling in cancer and approaches to enforce tumour regression. *Nature*. 441:437-443.

47. Shen, C., D. Nettleton, M. Jiang, S.K. Kim, and J.A. Powell-Coffman. 2005. Roles of the HIF-1 hypoxia-inducible factor during hypoxia response in Caenorhabditis elegans. *J Biol Chem*. 280:20580-20588.

48. Welch, W.J. 1993. Heat shock proteins functioning as molecular chaperones: their roles in normal and stressed cells. *Philos Trans R Soc Lond B Biol Sci*. 339:327-333.

49. Westwood, J.T., J. Clos, and C. Wu. 1991. Stress-induced oligomerization and chromosomal relocalization of heat-shock factor. *Nature*. 353:822-827.

50. Wu, C. 1995. Heat shock transcription factors: structure and regulation. *Annu Rev Cell Dev Biol*. 11:441-469.

51. Orosz, A., J. Wisniewski, and C. Wu. 1996. Regulation of Drosophila heat shock factor trimerization: global sequence requirements and independence of nuclear localization. *Mol Cell Biol*. 16:7018-7030.

52. Pelham, H.R. 1982. A regulatory upstream promoter element in the Drosophila hsp 70 heat-shock gene. *Cell*. 30:517-528.

53. Nambu, J.R., W. Chen, S. Hu, and S.T. Crews. 1996. The Drosophila melanogaster similar bHLH-PAS gene encodes a protein related to human hypoxia-inducible factor 1 alpha and Drosophila single-minded. *Gene*. 172:249-254.

54. Semenza, G.L., B.H. Jiang, S.W. Leung, R. Passantino, J.P. Concordet, P. Maire, and A. Giallongo. 1996. Hypoxia response elements in the aldolase A, enolase 1, and lactate dehydrogenase A gene promoters contain essential binding sites for hypoxia-inducible factor 1. *J Biol Chem*. 271:32529-32537.

55. Aprelikova, O., G.V. Chandramouli, M. Wood, J.R. Vasselli, J. Riss, J.K. Maranchie, W.M. Linehan, and J.C. Barrett. 2004. Regulation of HIF prolyl hydroxylases by hypoxia-inducible factors. *J Cell Biochem*. 92:491-501.

56. Bray, N., and L. Pachter. 2004. MAVID: constrained ancestral alignment of multiple sequences. *Genome Res*. 14:693-699.

57. Barolo, S., L.A. Carver, and J.W. Posakony. 2000. GFP and beta-galactosidase transformation vectors for promoter/enhancer analysis in Drosophila. *Biotechniques*. 29:726, 728, 730, 732.

58. Gorr, T.A., T. Tomita, P. Wappner, and H.F. Bunn. 2004. Regulation of Drosophila hypoxia-inducible factor (HIF) activity in SL2 cells: identification of a hypoxia-induced variant isoform of the HIFalpha homolog gene similar. *J Biol Chem*. 279:36048-36058.

59. Jedlicka, P., M.A. Mortin, and C. Wu. 1997. Multiple functions of Drosophila heat shock transcription factor in vivo. *EMBO J*. 16:2452-2462.

60. Donnelly, T.J., R.E. Sievers, F.L. Vissern, W.J. Welch, and C.L. Wolfe. 1992. Heat shock protein induction in rat hearts. A role for improved myocardial salvage after ischemia and reperfusion? *Circulation*. 85:769-778.

61. Kabakov, A.E., K.R. Budagova, A.L. Bryantsev, and D.S. Latchman. 2003. Heat shock protein 70 or heat shock protein 27 overexpressed in human endothelial cells during posthypoxic reoxygenation can protect from delayed apoptosis. *Cell Stress Chaperones*. 8:335-347.

62. Morimoto, R.I. 1993. Cells in stress: transcriptional activation of heat shock genes. *Science*. 259:1409-1410.

63. Zelzer, E., Y. Levy, C. Kahana, B.Z. Shilo, M. Rubinstein, and B. Cohen. 1998. Insulin induces transcription of target genes through the hypoxia-inducible factor HIF-1alpha/ARNT. *EMBO J*. 17:5085-5094.

64. Mottet, D., V. Dumont, Y. Deccache, C. Demazy, N. Ninane, M. Raes, and C. Michiels. 2003. Regulation of hypoxia-inducible factor-1alpha protein level during hypoxic conditions by the phosphatidylinositol 3-kinase/Akt/glycogen synthase kinase 3beta pathway in HepG2 cells. *J Biol Chem*. 278:31277-31285.

65. Isaacs, J.S., Y.J. Jung, E.G. Mimnaugh, A. Martinez, F. Cuttitta, and L.M. Neckers. 2002. Hsp90 regulates a von Hippel Lindau-independent hypoxia-inducible factor-1 alpha-degradative pathway. *J Biol Chem*. 277:29936-29944.

66. Minet, E., D. Mottet, G. Michel, I. Roland, M. Raes, J. Remacle, and C. Michiels. 1999. Hypoxia-induced activation of HIF-1: role of HIF-1alpha-Hsp90 interaction. *FEBS Lett*. 460:251-256.

67. Maloyan, A., L. Eli-Berchoer, G.L. Semenza, G. Gerstenblith, M.D. Stern, and M. Horowitz. 2005. HIF-1alpha-targeted pathways are activated by heat acclimation

and contribute to acclimation-ischemic cross-tolerance in the heart. *Physiol Genomics*. 23:79-88.

68. Treinin, M., J. Shliar, H. Jiang, J.A. Powell-Coffman, Z. Bromberg, and M. Horowitz. 2003. HIF-1 is required for heat acclimation in the nematode Caenorhabditis elegans. *Physiol Genomics*. 14:17-24.

69. Nakano, M., D.L. Mann, and A.A. Knowlton. 1997. Blocking the endogenous increase in HSP 72 increases susceptibility to hypoxia and reoxygenation in isolated adult feline cardiocytes. *Circulation*. 95:1523-1531.

70. Ciocca, D.R., and S.K. Calderwood. 2005. Heat shock proteins in cancer: diagnostic, prognostic, predictive, and treatment implications. *Cell Stress Chaperones*. 10:86-103.

71. Clemens, J.C., C.A. Worby, N. Simonson-Leff, M. Muda, T. Maehama, B.A. Hemmings, and J.E. Dixon. 2000. Use of double-stranded RNA interference in Drosophila cell lines to dissect signal transduction pathways. *Proc Natl Acad Sci U S A*. 97:6499-6503.

72. Cherniack, N.S., and G.S. Longobardo. 1970. Oxygen and carbon dioxide gas stores of the body. *Physiol Rev*. 50:196-243.

73. Groenewegen, K.H., A.M. Schols, and E.F. Wouters. 2003. Mortality and mortality-related factors after hospitalization for acute exacerbation of COPD. *Chest*. 124:459-467.

74. Connors, A.F.J., N.V. Dawson, C. Thomas, F.E.J. Harrell, N. Desbiens, W.J. Fulkerson, P. Kussin, P. Bellamy, L. Goldman, and W.A. Knaus. 1996. Outcomes following acute exacerbation of severe chronic obstructive lung disease. The SUPPORT investigators (Study to Understand Prognoses and Preferences for Outcomes and Risks of Treatments). *Am J Respir Crit Care Med*. 154:959-967.

75. Hetherington, A.M., and J.A. Raven. 2005. The biology of carbon dioxide. *Curr Biol*. 15:R406-10.

76. Bahn, Y.S., and F.A. Muhlschlegel. 2006. CO2 sensing in fungi and beyond. *Curr Opin Microbiol*. 9:572-578.

77. Foley, E., and P.H. O'Farrell. 2003. Nitric oxide contributes to induction of innate immune responses to gram-negative bacteria in Drosophila. *Genes Dev*. 17:115-125.

78. Lemaitre, B., and J. Hoffmann. 2007. The host defense of Drosophila melanogaster. *Annu Rev Immunol*. 25:697-743.

79. Hoffmann, J.A., and J.M. Reichhart. 2002. Drosophila innate immunity: an evolutionary perspective. *Nat Immunol*. 3:121-126.

80. Goto, A., K. Matsushita, V. Gesellchen, L. El Chamy, D. Kuttenkeuler, O. Takeuchi, J.A. Hoffmann, S. Akira, M. Boutros, and J.M. Reichhart. 2008. Akirins are highly conserved nuclear proteins required for NF-kappaB-dependent gene expression in drosophila and mice. *Nat Immunol*. 9:97-104.

81. Li, G., D. Zhou, A.G. Vicencio, J. Ryu, J. Xue, A. Kanaan, O. Gavrialov, and G.G. Haddad. 2006. Effect of carbon dioxide on neonatal mouse lung: a genomic approach. *J Appl Physiol*. 101:1556-1564.

82. Jones, W.D., P. Cayirlioglu, I.G. Kadow, and L.B. Vosshall. 2007. Two chemosensory receptors together mediate carbon dioxide detection in Drosophila. *Nature*. 445:86-90.

83. Kwon, J.Y., A. Dahanukar, L.A. Weiss, and J.R. Carlson. 2007. The molecular basis of CO2 reception in Drosophila. *Proc Natl Acad Sci U S A*. 104:3574-3578.

84. Vadasz, I., L.A. Dada, A. Briva, H.E. Trejo, L.C. Welch, J. Chen, P.T. Toth, E. Lecuona, L.A. Witters, P.T. Schumacker, N.S. Chandel, W. Seeger, and J.I. Sznajder. 2008. AMP-activated protein kinase regulates CO2-induced alveolar epithelial dysfunction in rats and human cells by promoting Na,K-ATPase endocytosis. *J Clin Invest*. 118:752-762.

85. Sethi, S., and T.F. Murphy. 2001. Bacterial infection in chronic obstructive pulmonary disease in 2000: a state-of-the-art review. *Clin Microbiol Rev*. 14:336-363.

86. Shirasu-Hiza, M.M., and D.S. Schneider. 2007. Confronting physiology: how do infected flies die? *Cell Microbiol*. 9:2775-2783.

87. Cox, C.R., and M.S. Gilmore. 2007. Native microbial colonization of Drosophila melanogaster and its use as a model of Enterococcus faecalis pathogenesis. *Infect Immun*. 75:1565-1576.

88. Sethi, S. 2004. Bacteria in exacerbations of chronic obstructive pulmonary disease: phenomenon or epiphenomenon? *Proc Am Thorac Soc*. 1:109-114.

89. Schneider, D.S. 2007. How and why does a fly turn its immune system off? *PLoS Biol*. 5:e247.

90. Bogdan, C. 2001. Nitric oxide and the immune response. *Nat Immunol*. 2:907-916.

91. Lang, J.D.J., P. Chumley, J.P. Eiserich, A. Estevez, T. Bamberg, A. Adhami, J. Crow, and B.A. Freeman. 2000. Hypercapnia induces injury to alveolar epithelial cells via a nitric oxide-dependent pathway. *Am J Physiol Lung Cell Mol Physiol.* 279:L994-1002.

92. Lang, J.D., M. Figueroa, K.D. Sanders, M. Aslan, Y. Liu, P. Chumley, and B.A. Freeman. 2005. Hypercapnia via reduced rate and tidal volume contributes to lipopolysaccharide-induced lung injury. *Am J Respir Crit Care Med.* 171:147-157.

93. Briva, A., I. Vadasz, E. Lecuona, L.C. Welch, J. Chen, L.A. Dada, H.E. Trejo, V. Dumasius, Z.S. Azzam, P.M. Myrianthefs, D. Batlle, Y. Gruenbaum, and J.I. Sznajder. 2007. High CO2 levels impair alveolar epithelial function independently of pH. *PLoS ONE.* 2:e1238.

94. Choe, K.M., H. Lee, and K.V. Anderson. 2005. Drosophila peptidoglycan recognition protein LC (PGRP-LC) acts as a signal-transducing innate immune receptor. *Proc Natl Acad Sci U S A.* 102:1122-1126.

95. Ramet, M., P. Manfruelli, A. Pearson, B. Mathey-Prevot, and R.A. Ezekowitz. 2002. Functional genomic analysis of phagocytosis and identification of a Drosophila receptor for E. coli. *Nature.* 416:644-648.

96. Stoven, S., I. Ando, L. Kadalayil, Y. Engstrom, and D. Hultmark. 2000. Activation of the Drosophila NF-kappaB factor Relish by rapid endoproteolytic cleavage. *EMBO Rep.* 1:347-352.

97. Ni Chonghaile, M., B. Higgins, and J.G. Laffey. 2005. Permissive hypercapnia: role in protective lung ventilatory strategies. *Curr Opin Crit Care.* 11:56-62.

98. Vittimberga, F.J.J., D.P. Foley, W.C. Meyers, and M.P. Callery. 1998. Laparoscopic surgery and the systemic immune response. *Ann Surg.* 227:326-334.

99. O'Croinin, D.F., A.D. Nichol, N. Hopkins, J. Boylan, S. O'Brien, C. O'Connor, J.G. Laffey, and P. McLoughlin. 2008. Sustained hypercapnic acidosis during pulmonary infection increases bacterial load and worsens lung injury. *Crit Care Med.* 36:2128-2135.

100. Margulies, M., M. Egholm, W.E. Altman, S. Attiya, J.S. Bader, L.A. Bemben, J. Berka, M.S. Braverman, Y.J. Chen, Z. Chen, S.B. Dewell, L. Du, J.M. Fierro, X.V. Gomes, B.C. Godwin, W. He, S. Helgesen, C.H. Ho, G.P. Irzyk, S.C. Jando, M.L. Alenquer, T.P. Jarvie, K.B. Jirage, J.B. Kim, J.R. Knight, J.R. Lanza, J.H. Leamon, S.M. Lefkowitz, M. Lei, J. Li, K.L. Lohman, H. Lu, V.B. Makhijani, K.E. McDade, M.P. McKenna, E.W. Myers, E. Nickerson, J.R. Nobile, R. Plant, B.P. Puc, M.T. Ronan, G.T. Roth, G.J. Sarkis, J.F. Simons, J.W. Simpson, M. Srinivasan, K.R. Tartaro, A. Tomasz, K.A. Vogt, G.A. Volkmer, S.H. Wang, Y. Wang, M.P. Weiner,

P. Yu, R.F. Begley, and J.M. Rothberg. 2005. Genome sequencing in microfabricated high-density picolitre reactors. *Nature*. 437:376-380.

101. Bennett, S. 2004. Solexa Ltd. *Pharmacogenomics*. 5:433-438.

102. Mangiapan, G., M. Vokurka, L. Schouls, J. Cadranel, D. Lecossier, J. van Embden, and A.J. Hance. 1996. Sequence capture-PCR improves detection of mycobacterial DNA in clinical specimens. *J Clin Microbiol*. 34:1209-1215.

103. Meyer, Q.C., S.G. Burton, and D.A. Cowan. 2007. Subtractive hybridization magnetic bead capture: a new technique for the recovery of full-length ORFs from the metagenome. *Biotechnol J*. 2:36-40.

104. Bashiardes, S., R. Veile, C. Helms, E.R. Mardis, A.M. Bowcock, and M. Lovett. 2005. Direct genomic selection. *Nat Methods*. 2:63-69.

105. St John, J., and T.W. Quinn. 2008. Rapid capture of DNA targets. *Biotechniques*. 44:259-264.